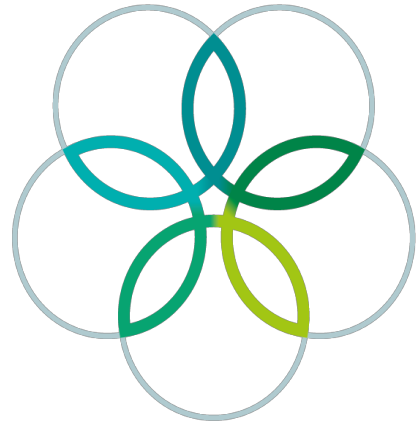
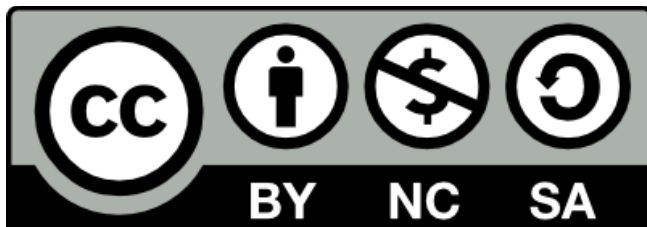


INTERNATIONAL
BIOLOGY
OLYMPIAD e. V.

IBO



All IBO examination questions are published under the following Creative Commons license:



CC BY-NC-SA (Attribution-NonCommercial-ShareAlike) -
<https://creativecommons.org/licenses/by-nc-sa/4.0/>

The exam papers can be used freely for educational purposes as long as IBO is credited and new creations are licensed under identical terms. No commercial use is allowed.

IBO 2018: Theoretical exam 2

Duration

This exam lasts three hours.

Topics

Q 1–16 Biochemistry and cell biology

Q 17–31 Animal physiology and anatomy

Q 32–40 Plant physiology

Q 41–51 Ecology and evolution

Marking

For questions with four statements the following marking scheme is used:

Number of correct answers	0	1	2	3	4
Points	0	0	0	0.5	1.0

For questions with five statements the following marking scheme is used:

Number of correct answers	0	1	2	3	4	5
Points	0	0	0	0.25	0.75	1.25

Original version: IBO 2018 Scientific Committee (Teheran, Iran)

Date: December 1, 2018

Editor: Roel Baars, The Netherlands

This edited version contains typographical, textual and graphical corrections compared with the original exam. This version was approved by the main organizers of IBO 2018.

Q. 1 – Linkage

The HapMap project was designed to estimate the amount of variation among the genomes of different individuals. One of the outcomes of the project was identification of many SNPs (single nucleotide polymorphisms) in the human genome. It was observed that the vast majority (here, assume all) of SNPs exist as only one of two (not four) nucleotides.

Therefore, for a region of the genome consisting of n SNPs, 2^n combinations of the SNPs are conceivable. In fact, sequencing of the SNPs in hundreds of individuals has revealed that generally a much lower number of combinations exist. The combinations of SNPs in fact observed in a region of the genome are named the SNP haplotypes of that region. The figure below is a representation of this finding. It shows the genotype of 26 neighbouring SNPs in a region of human chromosome 5 from 20 individuals of different populations throughout the world. Only one copy of chromosome 5 was isolated from each individual. The chromosomes are grouped on basis of having the same combination of genotypes for all the SNPs (i.e. having the same haplotype).

Chromosomal haplotype	I					II				III				IV			V		VI	VI
Individual	1	2	3	4	5	6	7	8	9	10	11	12	13	14	15	16	17	18	19	20
SNP No.																				
1	X	X	X	X	X	O	O	O	O	O	O	O	O	X	X	X	O	O	X	X
2	X	X	X	X	X	O	O	O	O	X	X	X	X	X	X	X	X	X	X	X
3	X	X	X	X	X	O	O	O	O	X	X	X	X	X	X	X	X	X	O	O
4	X	X	X	X	X	O	O	O	O	X	X	X	X	X	X	X	X	X	X	X
5	X	X	X	X	X	O	O	O	O	X	X	X	X	X	X	X	X	X	O	X
6	X	X	X	X	X	O	O	O	O	X	X	X	X	X	X	X	X	X	O	X
7	X	X	X	X	X	O	O	O	O	X	X	X	X	X	X	X	X	X	X	X
8	O	O	O	O	O	O	O	O	O	X	X	X	X	X	X	X	X	X	O	O
9	X	X	X	X	X	O	O	O	O	X	X	X	X	X	X	X	X	X	X	X
10	X	X	X	X	X	X	X	X	X	X	X	X	X	X	X	X	O	O	O	X
11	O	O	O	O	O	X	X	X	X	X	X	X	X	X	X	X	X	X	X	X
12	X	X	X	X	X	X	X	X	X	O	O	O	O	X	X	X	O	O	X	O
13	X	X	X	X	X	O	O	O	O	X	X	X	X	X	X	X	X	X	X	X
14	X	X	X	X	X	X	X	X	X	O	O	O	O	X	X	X	O	O	X	X
15	X	X	X	X	X	X	X	X	X	O	O	O	O	X	X	X	O	O	X	X
16	O	O	O	O	O	X	X	X	X	X	X	X	X	X	X	X	O	O	X	X
17	X	X	X	X	X	X	X	X	X	O	O	O	O	X	X	X	O	O	X	X
18	X	X	X	X	X	X	X	X	X	O	O	O	O	X	X	X	O	O	X	O
19	O	O	O	O	O	X	X	X	X	X	X	X	X	O	O	O	X	X	O	X
20	O	O	O	O	O	X	X	X	X	X	X	X	X	X	X	X	X	X	X	X
21	X	X	X	X	X	O	O	O	O	X	X	X	X	X	X	X	X	X	O	X
22	O	O	O	O	O	X	X	X	X	X	X	X	X	X	X	X	X	X	X	O
23	X	X	X	X	X	X	X	X	X	O	O	O	O	O	O	O	O	O	X	X
24	X	X	X	X	X	O	O	O	O	X	X	X	X	X	X	X	X	X	X	X
25	O	O	O	O	O	X	X	X	X	X	X	X	X	X	X	X	X	X	X	O
26	O	O	O	O	O	X	X	X	X	X	X	X	X	X	X	X	X	X	X	X

Genotype of 26 linked SNPs in the human genome on 20 copies of chromosome 5 from 20 individuals. X and O represent the two different nucleotides at each SNP position.

- | | True | False |
|--|--------------------------|--------------------------|
| A. Recombination events are not expected to affect the number of haplotypes observed in a population. | <input type="checkbox"/> | <input type="checkbox"/> |
| B. If in fact all conceivable haplotypes of the 26 SNPs analysed were present in the human population, one would not expect any two of the 20 chromosomes analysed to have the same haplotype. | <input type="checkbox"/> | <input type="checkbox"/> |
| C. Based on data presented in the table, knowledge of the nucleotide at only SNP 19 and SNP 23 of chromosome 5 of newly investigated individuals from the same cohort would allow prediction of the most likely nucleotides present at the remaining 24 SNP positions of chromosome 5 of those individuals. | <input type="checkbox"/> | <input type="checkbox"/> |
| D. The data on the 20 chromosomes suggest that among the four major haplotypes, haplotype IV has the minimum number of sequence variations. | <input type="checkbox"/> | <input type="checkbox"/> |

Q. 2 – Berk-Sharp mapping

A protocol that can be used for identification of gene structure with respect to exons and introns involves isolation and denaturation of a dsDNA fragment that includes a gene of interest, isolation of mature mRNA pertaining to gene of interest, hybridization of complementary single stranded nucleic acid molecules, performance of three types of chemical or enzymatic reactions, and electrophoresis on non-denaturing gels. Relevant factors pertaining the chemical or enzymatic reactions are as follows:

- S1: a nuclease that degrades single stranded (ss) nucleic acid molecules or regions that are single stranded. It does not degrade double stranded (ds) molecules or double stranded regions.
- Exonuclease VII: an exonuclease that degrades ss nucleic acids or ss ends of hybridized nucleic acids in both 5' to 3' and 3' to 5' directions. It does not degrade ds molecules or ds portions of molecules.
- Alkali conditions degrade RNA and do not degrade DNA.

Experiments pertaining to a gene that does not experience alternative splicing were as follows; appropriate size markers were included in the electrophoresis steps:

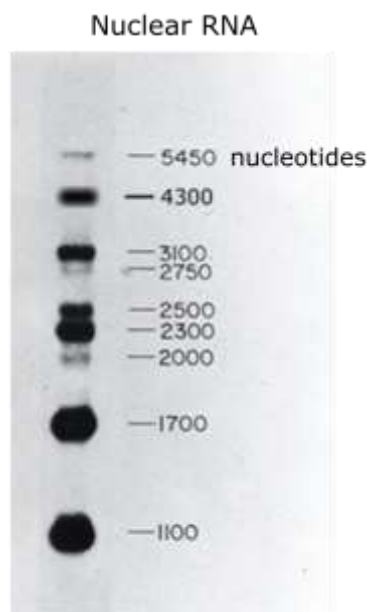
- Hybridization of denatured DNA with excess mRNA, followed by S1 treatment, followed by alkali treatment, followed by electrophoresis
- Hybridization of denatured DNA with excess mRNA, followed by S1 treatment, followed by electrophoresis
- Hybridization of denatured DNA with excess mRNA, followed by Exonuclease VII treatment, followed by alkali treatment, followed by electrophoresis

	True	False
A. Observation of three bands in electrophoresis pattern of reaction A signifies that the gene of interest has three exons.	<input type="checkbox"/>	<input type="checkbox"/>
B. The result of reaction A allows prediction of number and size of bands to be seen after electrophoresis in reaction B.	<input type="checkbox"/>	<input type="checkbox"/>
C. The result of reaction B allows estimation of size of gene of interest.	<input type="checkbox"/>	<input type="checkbox"/>
D. The combined results of reactions A and B allow prediction of the size of the introns of the gene.	<input type="checkbox"/>	<input type="checkbox"/>
E. The combined results of the three reactions A, B, and C will allow prediction of length of ORF (open reading frame) of gene of interest.	<input type="checkbox"/>	<input type="checkbox"/>

Q. 3 – mRNA Splicing

One of the questions that long ago arose with respect to splicing was whether the temporal order of removal of introns in transcripts of genes with multiple introns is the same as the physical order of the introns.

To address this question with respect to the ovomucoid encoding gene (5.6 Kbp) that has seven introns (A–G), Northern blotting was performed on RNA isolated from nuclei of ovomucoid expressing cells. The probe used in the Northern blotting was labelled DNA of the ovomucoid encoding gene. An image of the Northern blot is presented below. RNA was extracted from each major band seen in gel, and the presence or absence of specific introns in RNA molecules of various band was assessed using intron-specific probes. Finally, the RNA molecules were grouped on the basis of number of introns removed by splicing and calculations that revealed identity of introns lost in various processed RNA molecules were made. The results of these calculations are also presented below.



Northern blot

Intron removal from ovomucoid nuclear RNA

Frequency (%) of loss of individual introns

Group No.	Number of introns spliced out	A	B	C	D	E	F	G
1	2	5	0	0	0	30	60	5
2	2	25	25	0	5	60	60	25
3	3	5	5	5	30	100	95	60
4	4	10	25	35	95	90	90	55
5	5	40	75	65	85	100	75	60
6	6	50	100	75	90	100	100	75

- | | True | False |
|---|--------------------------|--------------------------|
| A. The image of the Northern blot suggests that order of removal of introns from ovomucoid primary transcripts is not random. | <input type="checkbox"/> | <input type="checkbox"/> |
| B. The data in the table show that intron E is usually but not always removed from primary transcripts before intron G is removed. | <input type="checkbox"/> | <input type="checkbox"/> |
| C. The data in the table indicate that introns A, B, and C are usually removed from primary transcripts before introns D and G. | <input type="checkbox"/> | <input type="checkbox"/> |
| D. The data presented suggest that at the time of analysis, there is generally a progressive increase in concentrations of more highly processed transcripts. | <input type="checkbox"/> | <input type="checkbox"/> |

Q. 4 – Inflammatory Caspases

Inflammatory caspases such as caspase 1 are activated in response to microbial infection and stress signals. When activated, they cleave human gasdermin D (GSDMD) after Asp275, to generate an N-terminal cleavage product (GSDMD-NT) and a C-terminal fragment (GSDMD-CT). GSDMD-NT kills bacteria and induces a form of programmed cell death called pyroptosis in human cells. The details of the mechanism by which GSDMD-NT causes cell death are unknown. Mutation of two evolutionarily conserved positively charged residues to alanine produces a mutant form of the protein known as GSDMD-NT 2A, and mutation of four conserved positively charged residues to alanine produces GSDMD-NT 4A. Fig. 1 shows result of non-reducing gel electrophoresis of equal amounts of N-terminal cleavage product of the wild type and mutated forms of GSDMD.

In an experiment, *E. coli* and *Staphylococcus aureus* bacteria were exposed to nanomolar concentrations of recombinant forms of GSDMD, GSDMD-NT, GSDMD-CT, GSDMD-NT 4A and granulysin (a known cytotoxic lymphocyte pore-forming protein) and the antibacterial effect of these molecules was assessed by measuring reduction of colony formation (Colony Forming Unit, CFU) (Fig. 2). Other experiments showed the same relative effects of the wild type and mutant forms on pyroptosis in human cells.

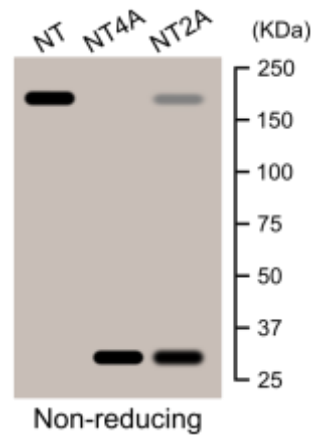


Figure 1

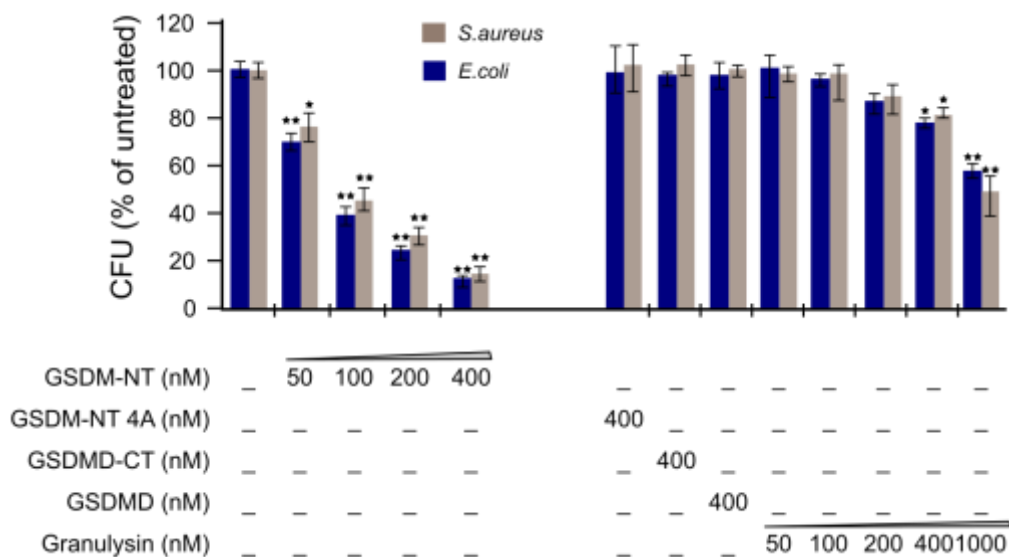
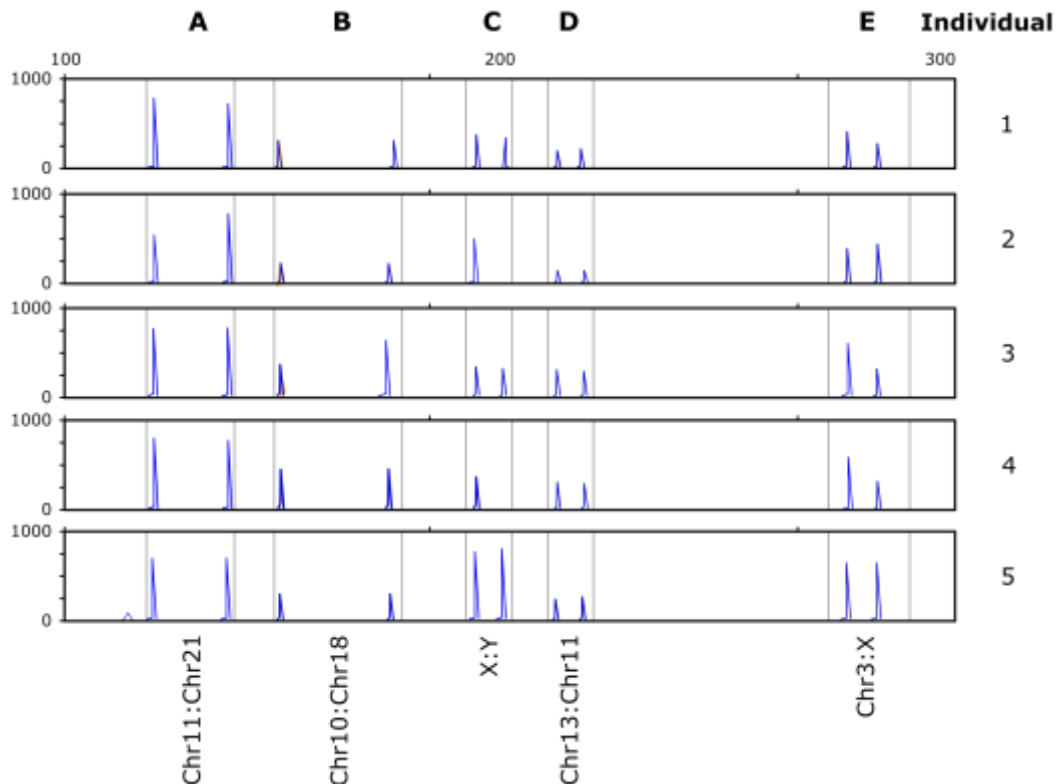


Figure 2

- | | True | False |
|---|--------------------------|--------------------------|
| A. The data shows that GSDMD-NT oligomerization is involved in pyroptosis. | <input type="checkbox"/> | <input type="checkbox"/> |
| B. GSDMD-NT is a more effective anti-bacterial agent than granulysin. | <input type="checkbox"/> | <input type="checkbox"/> |
| C. By mutation of evolutionarily conserved basic residues to Ala, the number of disulfide bonds between monomers of GSDMD does not change. | <input type="checkbox"/> | <input type="checkbox"/> |
| D. GSDMD-NT 2A mutant is likely less effective than GSDMD-NT for induction of pyroptosis. | <input type="checkbox"/> | <input type="checkbox"/> |

Q. 5 – Aneuploidy

Electrophoresis patterns of PCR products of several chromosome pairs (pairs shown on bottom) in five different individual (1–5) in figure below allow evaluation of presence or absence of chromosome number abnormality. Monosomy of autosomal chromosomes is known to be lethal. Relative height of the peaks in each box reflects the copy number ratio of the two chromosomes in that box. The horizontal axis shows migration, and the vertical axis shows fluorescence intensity.



A. Three individuals show trisomy.

B. Two individuals show abnormal monosomy.

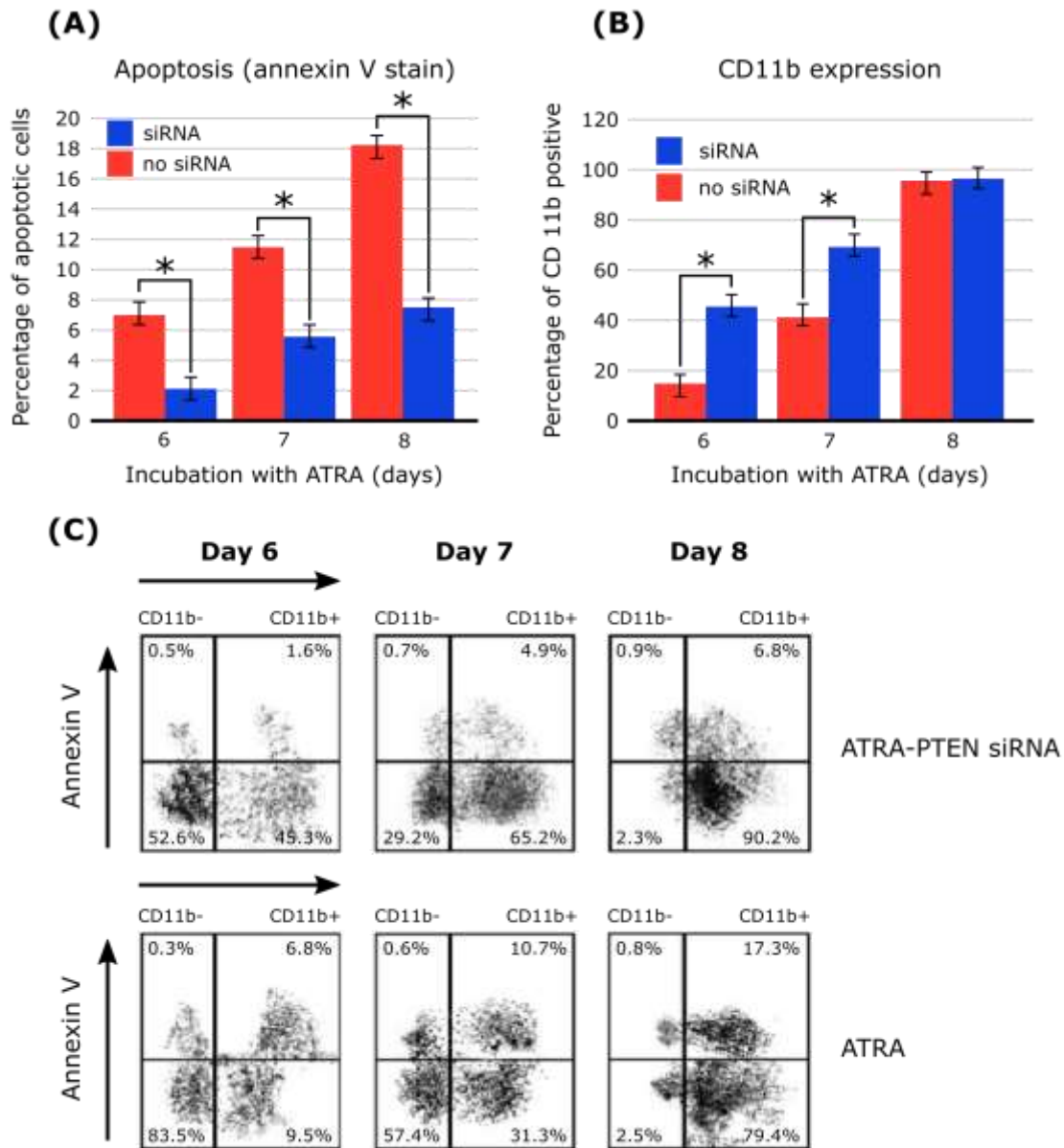
C. Two individuals have normal karyotypes.

D. PCR products related to different chromosomes should have different sizes to allow copy number evaluation.

True **False**

Q. 6 – Differentiation of Neutrophils

HL-60 cells differentiate to neutrophils after eight days of incubation in the presence of All Trans retinoic acid (ATRA). siRNAs are synthetic molecules used to suppress expression of genes. In the experiment whose results are presented below, an siRNA against the *PTEN* gene was used. Annexin V is a marker used to show apoptosis, and CD11b is a neutrophil surface marker. Percentage of apoptotic and differentiated cells as well as combination of both are shown in panels A, B and C. In panels A and B, stars indicate statistical significant.



(C) Horizontal line within each box reflects threshold value for apoptosis. Vertical line within each box reflects threshold value for neutrophil differentiation.

- | | True | False |
|---|--------------------------|--------------------------|
| A. The level of differentiation to neutrophils in the presence of <i>PTEN</i> siRNA is less than in the absence of <i>PTEN</i> siRNA at a statistically significant level. | <input type="checkbox"/> | <input type="checkbox"/> |
| B. Panels a and b show that reduction of apoptosis causes an increase in the number of live neutrophil cells at all time points. | <input type="checkbox"/> | <input type="checkbox"/> |
| C. Panel c shows an inverse correlation between apoptosis and the number of differentiated neutrophil cells at at least two time points. | <input type="checkbox"/> | <input type="checkbox"/> |
| D. <i>PTEN</i> siRNA applications causes larger reduction of apoptosis in differentiated cells as compared to undifferentiated cells after 7 days of incubation with ATRA. | <input type="checkbox"/> | <input type="checkbox"/> |

Q. 7 – Blood Types

Among 1290 individuals of a population under study, the numbers of individuals with blood group types M, MN, and N are, respectively, 340, 880, and 70.

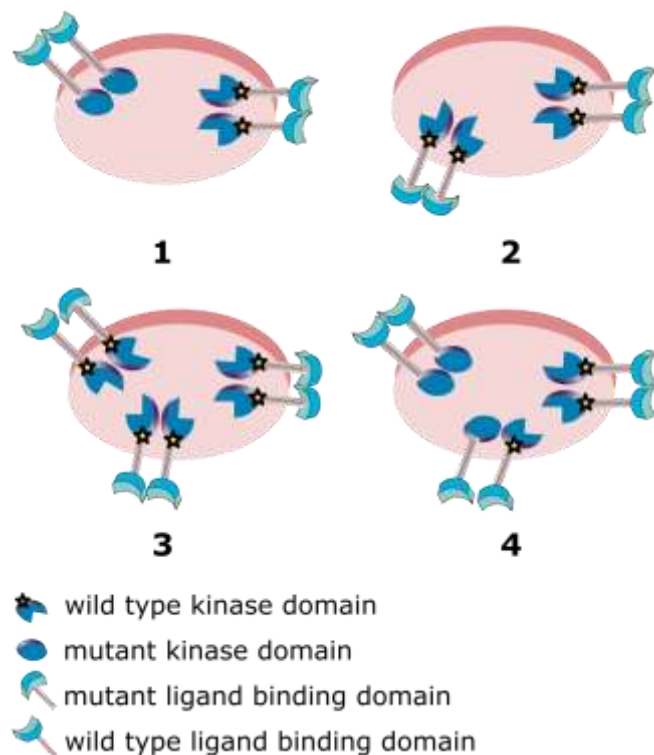
- | | True | False |
|---|--------------------------|--------------------------|
| A. Based on the data, the frequencies of M and N alleles in the population are, respectively, 0.7 and 0.3. | <input type="checkbox"/> | <input type="checkbox"/> |
| B. The population describe above is in Hardy Weinberg equilibrium with respect to alleles of the MN blood group. | <input type="checkbox"/> | <input type="checkbox"/> |
| C. If there is random mating in a population in which frequency of M alleles is 0.6 and frequency of N alleles is 0.4, the frequency of offspring with the NN genotype will be 0.16. | <input type="checkbox"/> | <input type="checkbox"/> |
| D. In a start generation with frequency of M = 0.6 and frequency of N = 0.4, after three generations of random mating the frequency of MM individuals in the population of the fourth generation who are offspring of MN*MN matings will be <10%. | <input type="checkbox"/> | <input type="checkbox"/> |

Q. 8 – Receptor Tyrosine Kinases

Two different mutant forms of a gene that encodes a cell surface receptor tyrosine kinase (RTK) are separately inserted into vectors. One mutant encodes a protein with a non-functional kinase domain, and the other lacks a functional ligand binding domain. Each vector is separately introduced into normal cells that can express wild type RTK from their endogenous genes.

It is known that the cells used have a high capacity for RTK receptors on their surface, that ligands bind to monomeric forms of receptor proteins and that heterodimeric receptors are inactive in signalling. The diagrams below depict four cell types identified. Each diagram shows the only receptor forms observed on the respective cell types in the ratio that they were observed.

The experiments were performed under non-saturating concentrations of ligand.

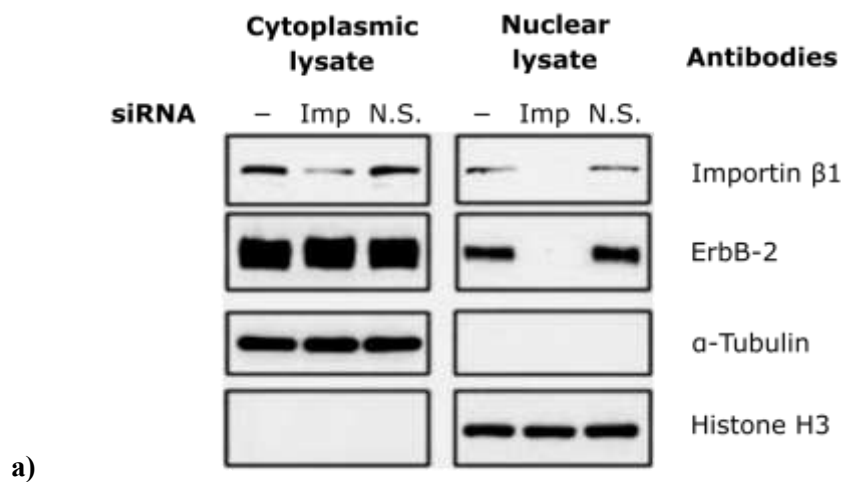


- | | True | False |
|--|--------------------------|--------------------------|
| A. In type 1 cells, the mutant receptor with the non-functional kinase domain will interfere with signalling by the cells' normal RTK. | <input type="checkbox"/> | <input type="checkbox"/> |
| B. In type 2 cells, the mutant RTK lacking functional ligand binding domain will be inactive for signalling, but will not interfere with normal signalling mediated by the cells' own receptor tyrosine kinases. | <input type="checkbox"/> | <input type="checkbox"/> |
| C. Equal levels of signalling will be achieved by type 3 and type 4 cells. | <input type="checkbox"/> | <input type="checkbox"/> |
| D. The effects of mutant RTKs of cell type 2 and cell type 3 on levels of signalling by the cells' own normal RTKs will be the same. | <input type="checkbox"/> | <input type="checkbox"/> |

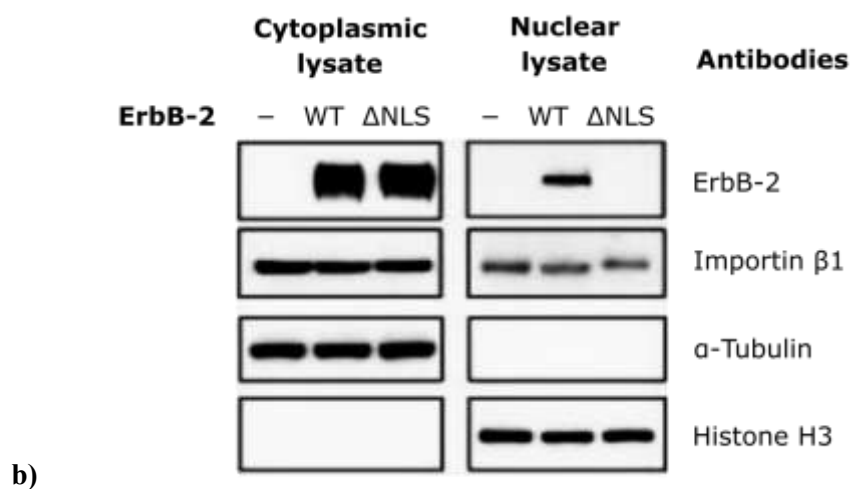
Q. 9 – ErbB-2 Transport

ErbB-2 is a receptor found on the plasma membrane of mammalian cells which can move from the plasma membrane to the nucleus. Because most proteins that shuttle between the cytoplasm and the nucleus are soluble and not integral membrane bound proteins, the mechanism by which ErbB-2 undergoes transport to the nucleus is of particular interest. Three experiments described below were done to shed light on the underlying mechanisms.

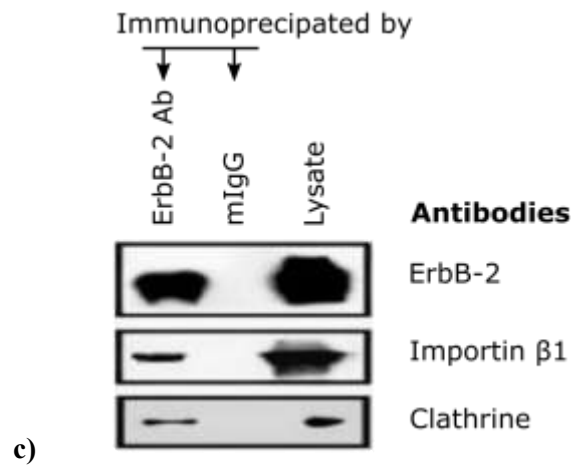
Experiment 1: siRNA knock down of importin β 1 expression in target cells. The cells were transfected with importin β 1 siRNA (Imp), non-functional siRNA control (N.S.), or buffer only (-). Proteins from the cytoplasmic and nuclear fraction of cell lysates were analysed by Western blotting using importin β 1, and ErbB-2, α tubulin and histone H3 antibodies as indicated.



Experiment 2: Mutant cells lacking ErbB-2 gene were transfected with wild-type ErbB-2 (WT), ErbB-2 mutant containing a deficient nuclear localization signal (Δ NLS), or vector control (-). Proteins from the cytoplasmic fraction, nuclear fraction were then analysed by Western blotting with ErbB-2, importin β 1, α tubulin and histone H3 antibodies as indicated.



Experiment 3: Cell lysates from the cells were immune-precipitated with anti-ErbB-2 or mouse IgG (mIgG). The precipitated immune-complexes and the cell lysates were then analysed by Western blotting with, clathrin, importin β 1, and ErbB-2 antibodies.



- | | True | False |
|---|--------------------------|--------------------------|
| A. The data in Figure (a) suggest that ErbB-2 requires importin β 1 in order to enter the nucleus. | <input type="checkbox"/> | <input type="checkbox"/> |
| B. It is predicted that the antibody against importin β 1 does not precipitate the ErbB-2(Δ NLS). | <input type="checkbox"/> | <input type="checkbox"/> |
| C. The data presented suggest that localization of histones to the nucleus is mediated by a mechanism distinct from that used to shuttle ErbB-2. | <input type="checkbox"/> | <input type="checkbox"/> |
| D. As true for other membrane bound receptors, ErbB2 enters the cytoplasm by endocytosis. | <input type="checkbox"/> | <input type="checkbox"/> |

Q. 10 – Yeast Secretion Trap

Phytopathogens use their secreted proteins “secretomes” to attack plant hosts. The yeast secretion trap (YST) functional screen is a method used for isolation and identification of these secreted proteins. This method involves generating a vector library that includes cDNAs (containing 5' non-coding sequences) synthesized using phytopathogen RNAs fused to a mutated form of the *Saccharomyces cerevisiae* *suc2* reporter gene.

Suc2 encodes invertase which is the only protein used by yeast for sucrose degradation. Degradation occurs in the extra-cellular medium. The mutated form of the gene *suc2*-SP encodes an invertase that lacks the signal peptide for secretion at the amino terminal. The fusion library is used to transfect an invertase-deficient yeast strain, and the cells are subsequently plated on a sucrose selection medium. Each rescued cell is expected to contain a recombinant vector whose cDNA that encodes a signal peptide for the chimeric protein. Vectors are isolated and their cDNAs are sequenced to identify the secreted proteins.

Figure 1 is a schematic presentation of the vector, and Figure 2 summarizes the protocol described above.

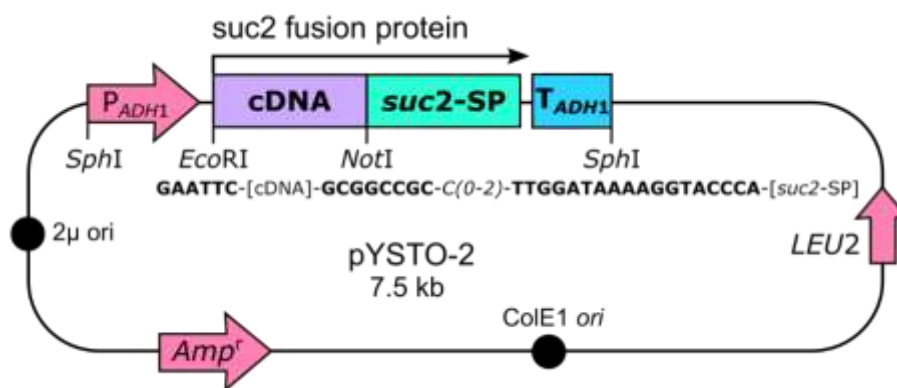


Figure 1. GAATTC: EcoR1 recognition site; GCGGCCGC: Not1 recognition site

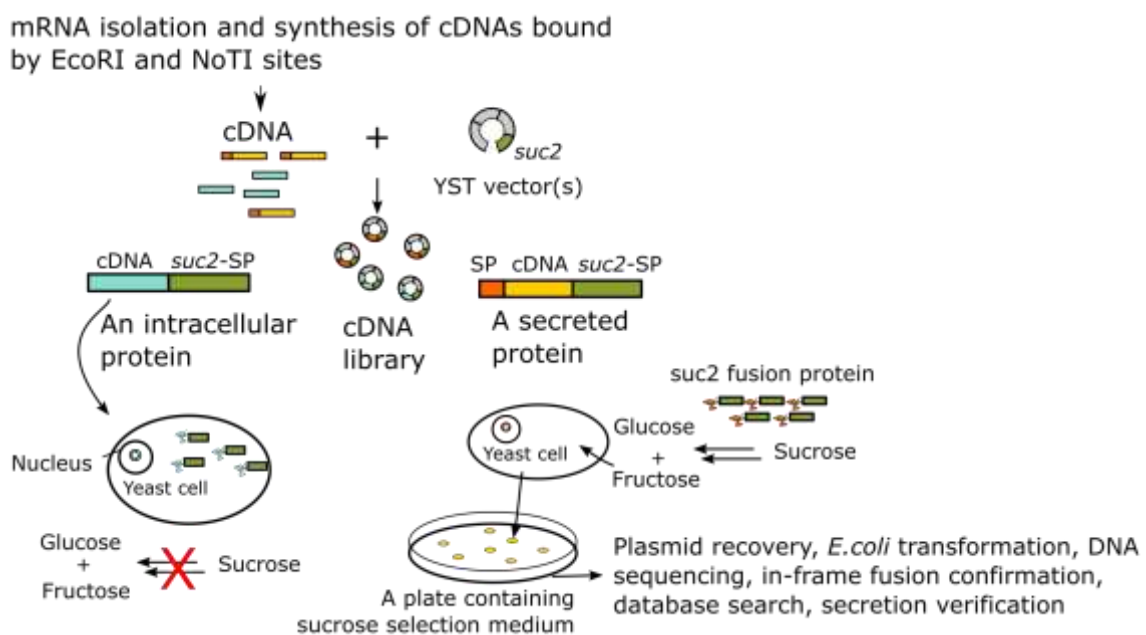


Figure 2.

- | | True | False |
|--|--------------------------|--------------------------|
| A. For the purpose of this screen, oligo-dT primers can be used for synthesis of cDNAs. | <input type="checkbox"/> | <input type="checkbox"/> |
| B. Variable number of Cytidine nucleotide(s) after the NotI site in the vector ensures achieving a correct reading frame. | <input type="checkbox"/> | <input type="checkbox"/> |
| C. Presence of signal peptide in the fusion protein will not necessarily ensure the growth of yeast on the selection medium. | <input type="checkbox"/> | <input type="checkbox"/> |
| D. For introduction of EcoRI and NotI sites to ends of cDNA molecules, linkers (which are short double stranded oligonucleotides; example shown below) are better than adapters (which have single stranded ends; example shown below). | <input type="checkbox"/> | <input type="checkbox"/> |

Example of EcoRI linker:

-GAATTC-

-CTTAAG-

Example of EcoRI adapters:

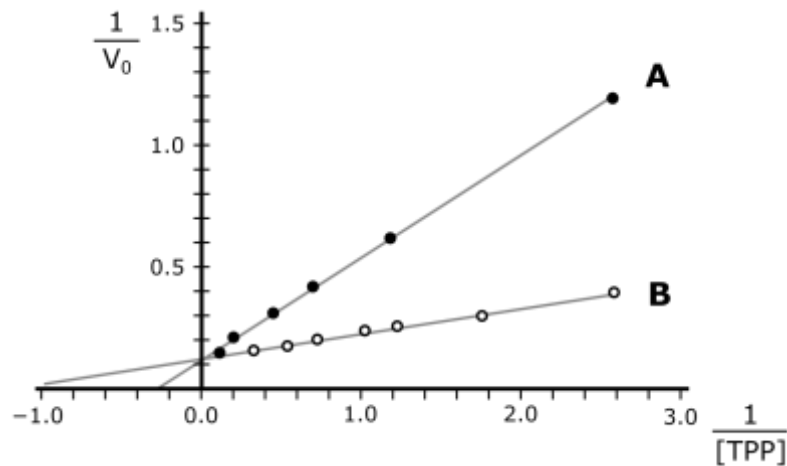
-G- and -AATTC-

-CTTAA- -G-

Q. 11 – Enzyme - Coenzyme Interaction

Many disease causing mutations in enzyme coding genes affect parameters related to interactions of the enzymes with their coenzyme, which in turn lowers the rate of the reaction. The cofactor of a group of enzymes called TPP- or thiamine-dependent enzymes such as transketolase is thiamine pyrophosphate (TPP).

The kinetic properties of a TPP-dependent enzyme isolated from a patient's tissue and a normal individual's tissue were compared under condition of substrate saturation. The TPP-free forms of the enzyme was prepared and used for enzyme kinetic measurements. The Lineweaver-Burk like plots are shown below.



- | | True | False |
|--|--------------------------|--------------------------|
| A. A is related to the patient's enzyme. | <input type="checkbox"/> | <input type="checkbox"/> |
| B. Maximum velocity of B is higher than the maximum velocity of A. | <input type="checkbox"/> | <input type="checkbox"/> |
| C. It can be concluded that the enzyme in A has a lower affinity for its substrate(s). | <input type="checkbox"/> | <input type="checkbox"/> |
| D. Administration of thiamine to patients is expected to restore enzymatic activity. | <input type="checkbox"/> | <input type="checkbox"/> |

Q. 12 – Förster Resonance Energy Transfer

Förster resonance energy transfer (FRET) is a distance-dependent process whereby energy from an excited fluorescent molecule (donor) is transferred to a second, non-excited molecule (acceptor) in its vicinity. The FRET efficiency depends on the spectral overlap of the donor emission spectrum and the acceptor absorption spectrum. Acceptors in various forms of FRET may or may not emit fluorescence after receipt of energy from donor.

Quantum dots (QDs) are fluorescent nanoparticles that can act as FRET donors and can be used in biosensor systems. The binding of some molecules to QDs enhances the emission properties of the QDs. In this study, 560 nm emitting QDs (QD-560) were used. Maltose Binding Protein (MBP)-bound QD-560 has higher emission than unbound QD-560.

The effect of native MBP or penta-histidine tagged MBP (MBP-5His) binding to QD-560 on fluorescence intensity was tested over a range of protein-to-QD ratios (Figure 1). Histidine residues can bind zinc ions present on the surface of the QD particles.

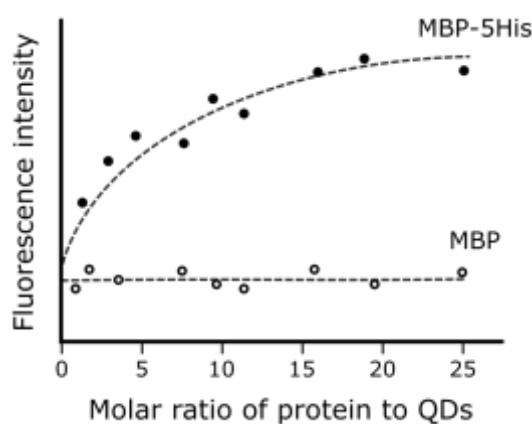


Figure 1: Fluorimetric measurements of QDs bound to MBPs or to MBP-5His at 560 nm.

For construction of a Maltose detecting biosensor, the saccharide binding pocket of each QD-coordinated MBP-5His was preloaded with a maltose analogue named β -cyclodextrin bound to QSY9 (β -CD-QSY9); the QSY9 component absorbs light. Figure 2 shows the biosensor.

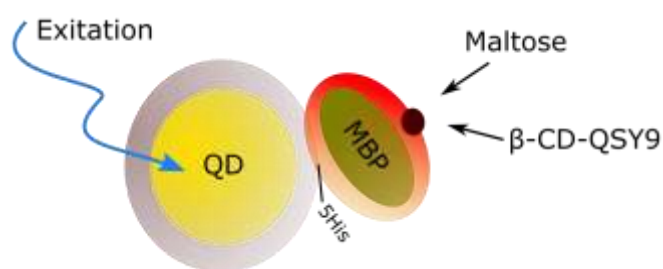


Figure 2: Schematic representation of maltose detecting biosensor.

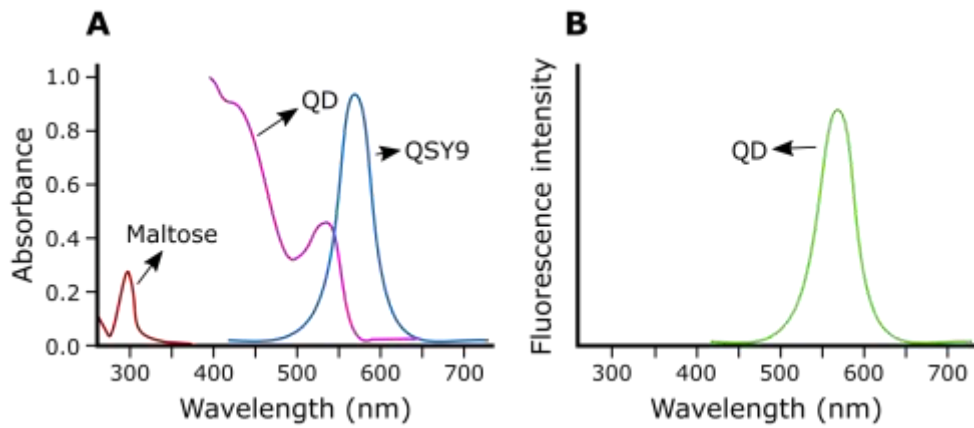
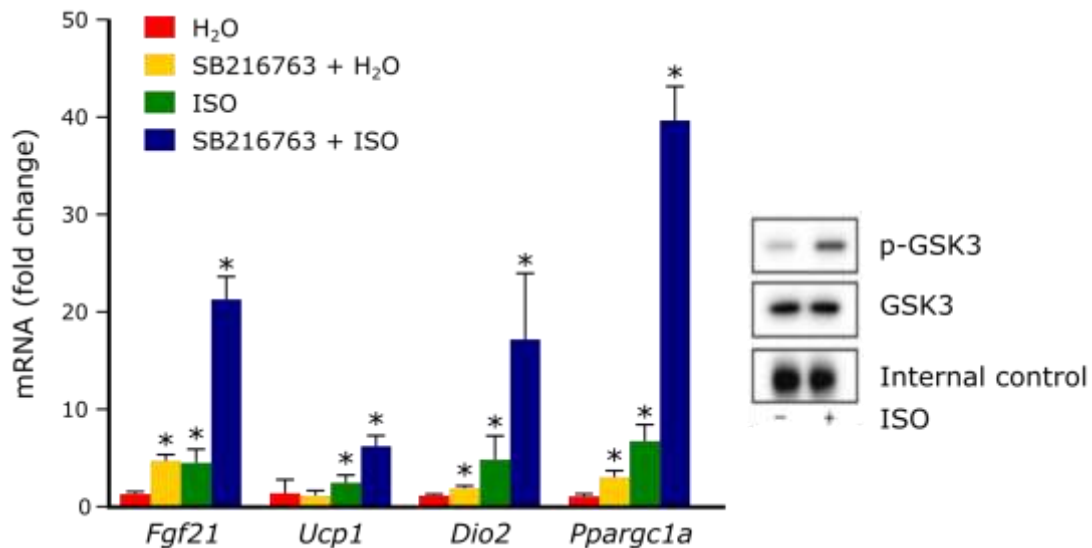


Figure 3: Absorption (A) and emission (B) spectra of various molecules.

- | | True | False |
|--|--------------------------|--------------------------|
| A. Displacement of β -CD-QSY9 by maltose on the biosensor will result in reduced fluorescence intensity. | <input type="checkbox"/> | <input type="checkbox"/> |
| B. In the absence of maltose, FRET cannot occur in the biosensor. | <input type="checkbox"/> | <input type="checkbox"/> |
| C. It is expected that relative fluorescence intensity levels under conditions below are
C > B > A
A: QD with MBP-5His and β -CD-QSY9 dye
B: QD with MBP-5His and free QSY9 dye
C: QD with MBP-5His | <input type="checkbox"/> | <input type="checkbox"/> |
| D. QD incubated with MBP that was preloaded with β -CD-QSY9 will not show FRET. | <input type="checkbox"/> | <input type="checkbox"/> |

Q. 13 – Expression of Thermogenic Genes

Brown adipose tissue (BAT) activation through β -adrenergic signalling pathway is associated with expression of thermogenic genes and the process of thermogenesis. Glycogen synthase kinase-3 (GSK3) acts as a regulator of β -adrenergic signalling in brown adipocytes. ISO is also a chemical stimulator of BAT activation; its effect on GSK3 is shown by the Western blot below (p-GSK3 is phosphorylated form of GSK3). SB216763 is an inhibitor of GSK3. Effects of these two agents on the expression of thermogenic genes (*Fgf21*, *Ucp1*, *Dio2*, and *Ppargc1a*) are shown in the Figure below.



(*) shows significant difference as compared to control (H₂O)

- A.** GSK3 acts as a negative regulator of β -adrenergic signalling in brown adipocytes.
- B.** Phosphorylation of GSK3 causes decreased expression of *Fgf21*.
- C.** SB216763 may prevent diet-induced obesity.
- D.** Use of SB216763 and ISO together cause much higher increase in the number of *Ppargc1a* mRNA transcripts as compared to *Fgf21* mRNA transcripts.

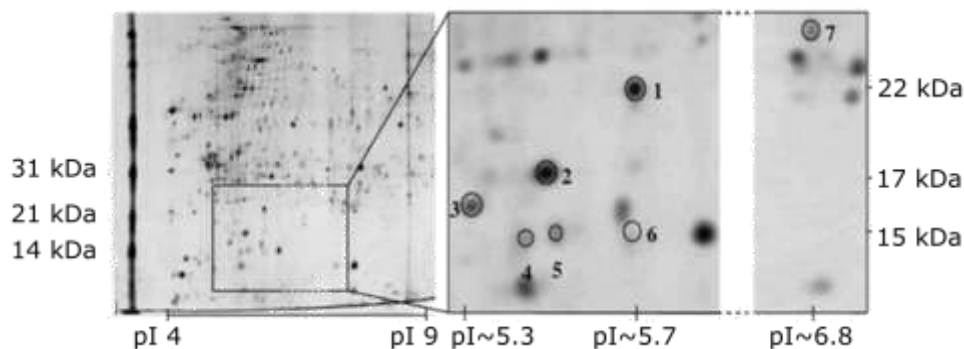
	True	False
A.	<input type="checkbox"/>	<input type="checkbox"/>
B.	<input type="checkbox"/>	<input type="checkbox"/>
C.	<input type="checkbox"/>	<input type="checkbox"/>
D.	<input type="checkbox"/>	<input type="checkbox"/>

Q. 14 – Antioxidant Defence in *Plasmodium*

Plasmodium is a parasitic protozoan that is prevalent in tropical countries. Once the parasites invade host red blood cells, they multiply within 24 h. Fe^{2+} in red blood cells can react with free O_2 as well as H_2O_2 , causing formation of free radicals that can damage parasite cells.

Unlike host cells, the parasites lack several enzymes of antioxidant defence systems. Scientists analysed the proteins from the parasite cytosol using two dimensional gel electrophoresis (see image below).

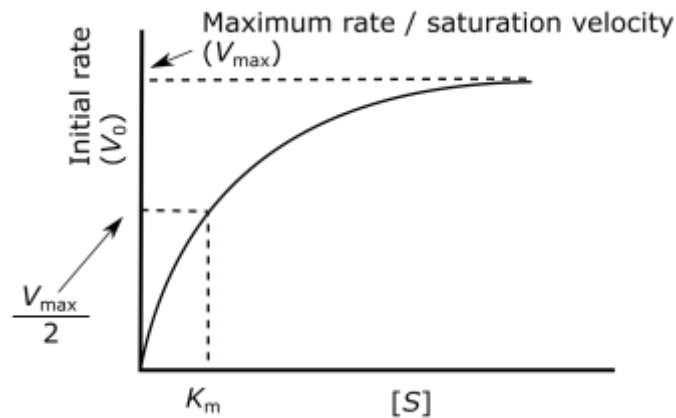
Then, using mass spectrometry and peptide mass fingerprinting, they identified 6 proteins (spots 1 to 6) corresponding to human peroxiredoxin, while one protein (spot 7) corresponding to *Plasmodium* peroxiredoxin.



- | | True | False |
|---|--------------------------|--------------------------|
| A. Based on the presented data, <i>Plasmodium</i> peroxiredoxin is a multimeric protein. | <input type="checkbox"/> | <input type="checkbox"/> |
| B. All human peroxiredoxin proteins have a positive net charge at physiological pH. | <input type="checkbox"/> | <input type="checkbox"/> |
| C. Gel filtration chromatography is suitable for separation and purification of the six human peroxiredoxin proteins. | <input type="checkbox"/> | <input type="checkbox"/> |
| D. Immunoaffinity chromatography can be used for separation of <i>Plasmodium</i> peroxiredoxin from other <i>Plasmodium</i> cytosolic proteins. | <input type="checkbox"/> | <input type="checkbox"/> |

Q. 15 – Enzyme Reaction Rate

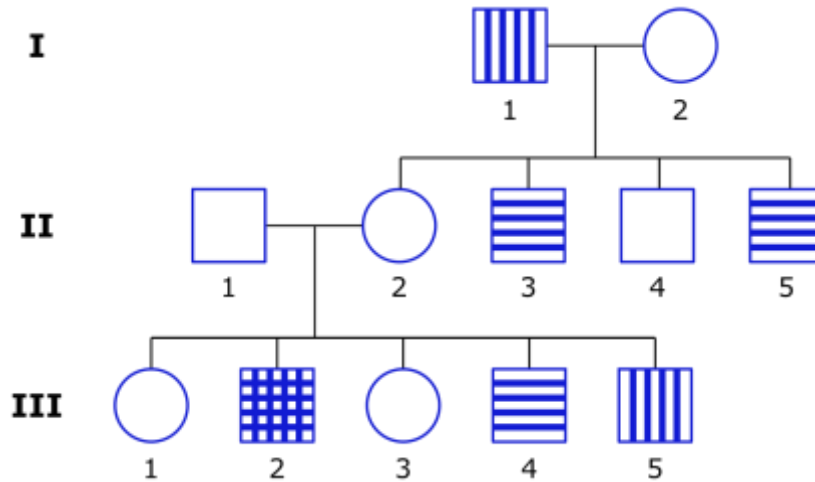
The figure below depicts the relation between substrate concentration and enzyme reaction rate.



- | | True | False |
|---|--------------------------|--------------------------|
| A. At saturating levels of substrate, the rate of an enzyme catalysed reaction is proportional to the enzyme concentration. | <input type="checkbox"/> | <input type="checkbox"/> |
| B. If enough substrate is added, the V_{\max} of an enzyme catalysed reaction in the presence of a non-competitive inhibitor can be the same as V_{\max} of the reaction in absence of the inhibitor. | <input type="checkbox"/> | <input type="checkbox"/> |
| C. The rate of an enzyme catalysed reaction in the presence of a rate-limiting concentration of substrate decreases with time. | <input type="checkbox"/> | <input type="checkbox"/> |
| D. The sigmoidal shape of the V versus $[S]$ curve obtained with allosteric enzymes indicates that the affinity of the enzyme for substrate decreases as the substrate concentration is increased. | <input type="checkbox"/> | <input type="checkbox"/> |
| E. The affinity of an allosteric enzyme for substrate varies with enzyme concentration. | <input type="checkbox"/> | <input type="checkbox"/> |

Q. 16 – Pedigree Analysis

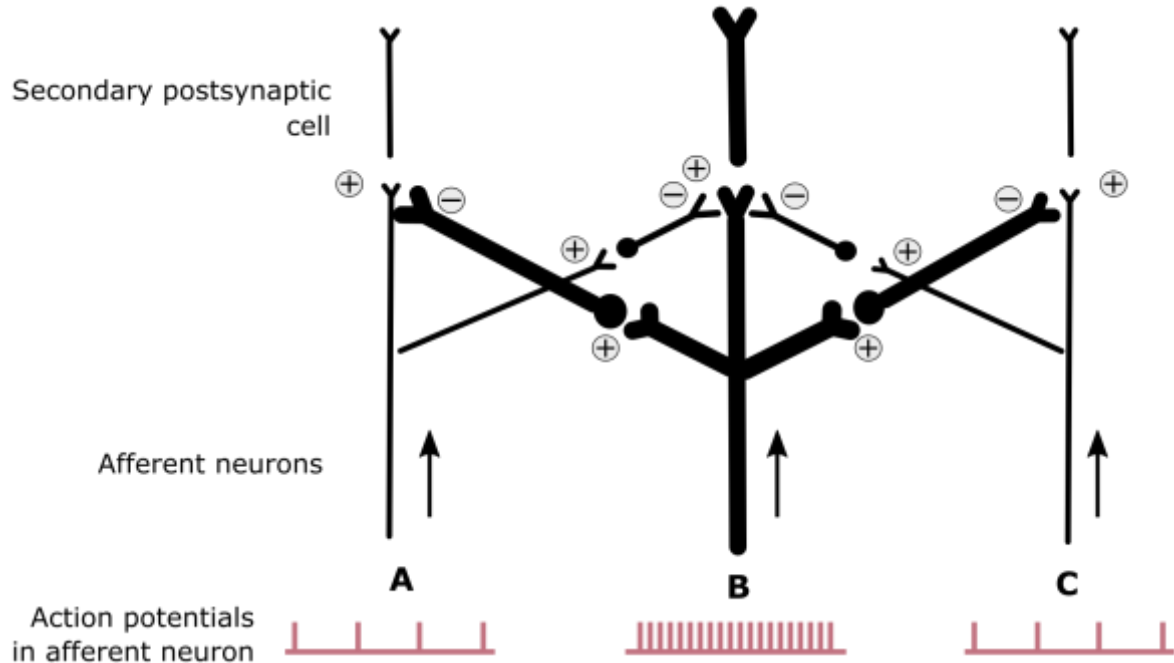
The inheritance pattern of two **rare** traits, represented as vertical and horizontal lines, is shown in the pedigree below.



- | | True | False |
|--|--------------------------|--------------------------|
| A. Inheritance of one of the traits is Y-linked. | <input type="checkbox"/> | <input type="checkbox"/> |
| B. The data presented is consistent with autosomal recessive inheritance for both traits. | <input type="checkbox"/> | <input type="checkbox"/> |
| C. The phenotype of III-2 may be due to non-disjunction in II-2. | <input type="checkbox"/> | <input type="checkbox"/> |
| D. The phenotype of III-2 may be due to cross over in II-2. | <input type="checkbox"/> | <input type="checkbox"/> |
| E. The probability of the phenotype of III-2 being due to a mutation that occurred in an egg cell of II-2 before fertilization is twice the probability of the phenotype of III-4 being due to a mutation that occurred in an egg cell of II-2 before fertilization. | <input type="checkbox"/> | <input type="checkbox"/> |

Q. 17 – Secondary Neurons

As it is shown in the figure, the sensory neurons can modify the function of adjacent sensory pathway. This inhibitory effect is conducted via intermediate neurons at their synapse with second-order neurons. The width of neurons is correlated with their activity.



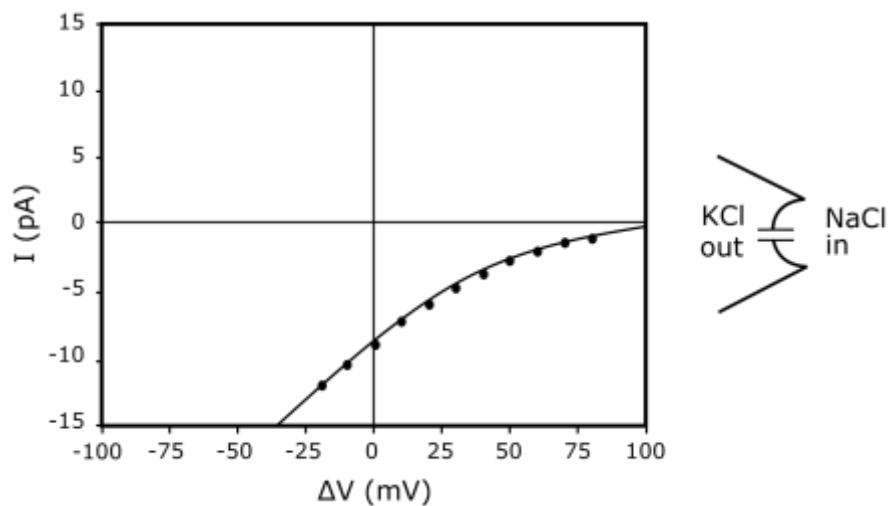
- | | True | False |
|---|--------------------------|--------------------------|
| A. The firing rate of all second-order neurons is higher than to first-order neurons. | <input type="checkbox"/> | <input type="checkbox"/> |
| B. The highest relative changes between second and first-order neurons will happen in Path B. | <input type="checkbox"/> | <input type="checkbox"/> |
| C. The difference between the firing rate of second order neurons in A and B pathways will be higher than the difference between firing rate of the first order neuron in these pathways. | <input type="checkbox"/> | <input type="checkbox"/> |
| D. This mechanism may help to localize the sensory stimulus more accurately. | <input type="checkbox"/> | <input type="checkbox"/> |

Q. 18 – Patch Clamp

A researcher used a patch clamp technique to record the current of only a cation channel (single channel recording). The pipette contains 150 mM of KCl surrounded by a bath solution containing 150 mM of NaCl, and measures the channel current by clamping the voltage in different values. Current-Voltage curve (I-V curve) is shown in the following figure. $\Delta V = V_{\text{interior}} - V_{\text{exterior}}$.

A negative current value (i.e., inward current) can reflect either the movement of positive ions (cations) into the cell or negative ions (anions) out of the cell.

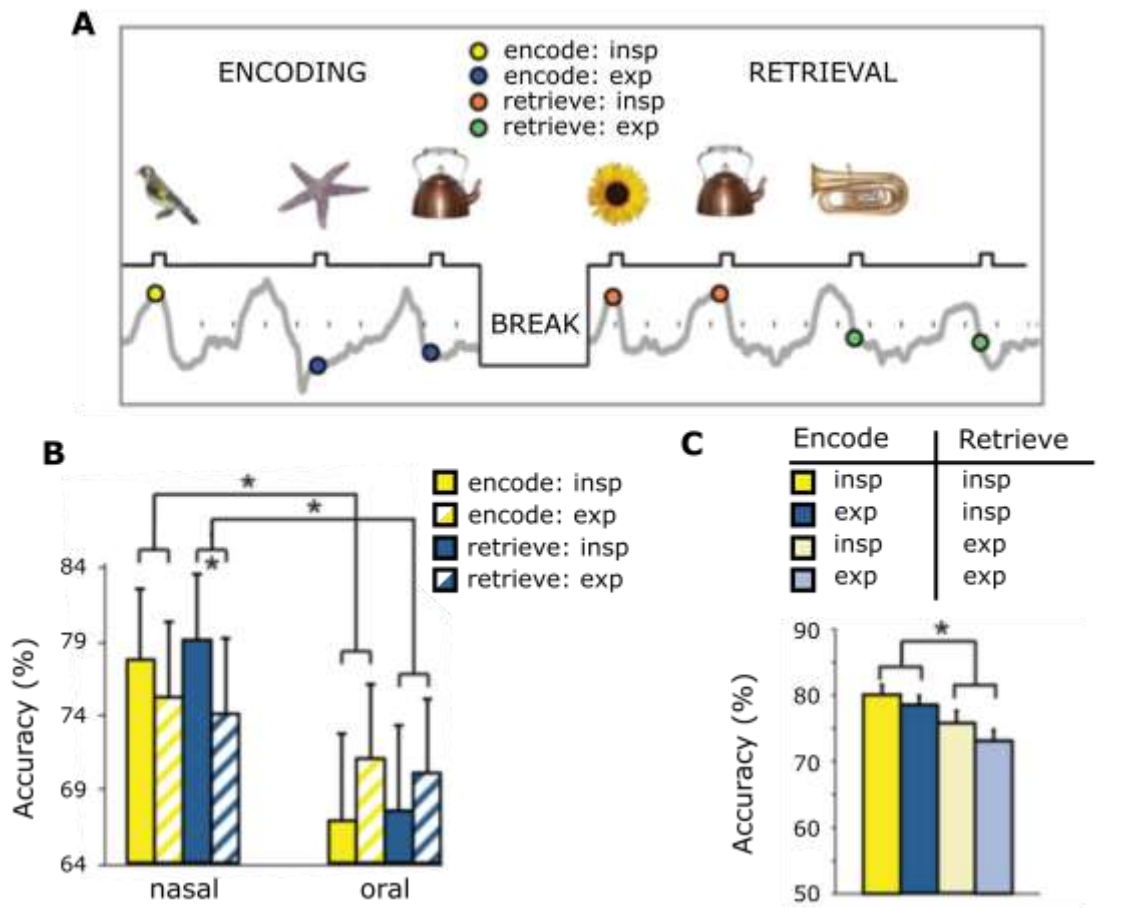
A positive current value (i.e., outward current) can reflect either the movement of positive ions (cations) out of the cell or negative ions (anions) into the cell.



- | | True | False |
|---|--------------------------|--------------------------|
| A. This channel is not selective, and both K^+ and Na^+ ions pass through this channel. | <input type="checkbox"/> | <input type="checkbox"/> |
| B. The Na^+ current decreases with increasing voltage. | <input type="checkbox"/> | <input type="checkbox"/> |
| C. The K^+ current increases with increasing voltage. | <input type="checkbox"/> | <input type="checkbox"/> |
| D. The resistance of the channel to negative voltages is less than positive voltages. | <input type="checkbox"/> | <input type="checkbox"/> |

Q. 19 – Memory Performance

In a recognition memory task, subjects (human being) viewed a series of different visual objects that occurred at different times within the breathing cycle. The interval between displaying images was 3–6 seconds. After a 20 min break, subjects were presented with the old pictures from the encoding session plus an equal number of new pictures; and the subjects pressed the “Yes” button if they had previously viewed the object’s image, and pressed the “No” button if the image was new. Subjects' memory performance was examined in the episodes of inspiration and expiration, and in mouth breathing and nasal breathing (In figures “*” means $p < 0.05$ which indicates significant difference between groups).



- | | True | False |
|---|--------------------------|--------------------------|
| A. The inspiration and expiration phase does not affect memory performance during oral breathing. | <input type="checkbox"/> | <input type="checkbox"/> |
| B. Memory function during nasal breathing is significantly more accurate than during oral breathing. | <input type="checkbox"/> | <input type="checkbox"/> |
| C. Regardless of the respiratory phase in which the image is encoded, if the object's images are depicted in the inspiration phase during the retrieval, memory performance is significantly greater. | <input type="checkbox"/> | <input type="checkbox"/> |
| D. In breathing through the nose, unlike encoding, the accuracy of retrieval in the inspiration phase is significantly higher than in the expiration phase. | <input type="checkbox"/> | <input type="checkbox"/> |

Q. 20 – Magnetic Resonance Imaging

The principle of magnetic resonance imaging (MRI) is based on the fact that the nuclei of certain elements align with the magnetic force when placed in a strong magnetic field. At the field strengths currently used in medical imaging, hydrogen nuclei (protons) in water molecules and lipids are responsible for producing anatomical images.

If a radiofrequency pulse at the resonant frequency of hydrogen is applied, a proportion of the protons change alignment, flipping through a present angle, and rotate in phase with one another. Following this radiofrequency pulse, the protons realign (relax), they induce a signal which, although very weak, can be detected and localized by copper coils placed around the patient. An image representing the distribution of the hydrogen protons can be built up.

The strength of the signal depends not only on proton density but also on two relaxation times, T1 and T2; T1 depends on the time the protons take to return to the axis of magnetic field, and T2 depends on the time the protons take to dephase. A T1-weighted image is one in which the contrast between tissues is due mainly to their T1 relaxation properties, while in a T2-weighted image the contrast is due to the T2 relaxation properties.

T1-weighted image: Fat signal intensity > Water signal intensity

T2-weighted image: Fat signal intensity < water signal intensity



Figure 1:
axial image
of brain

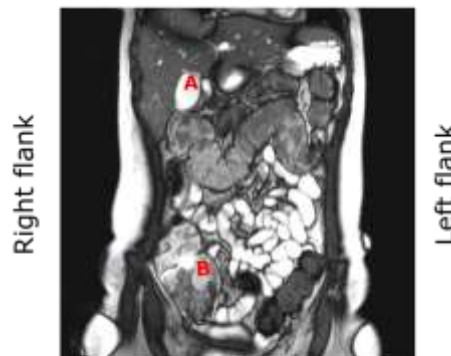
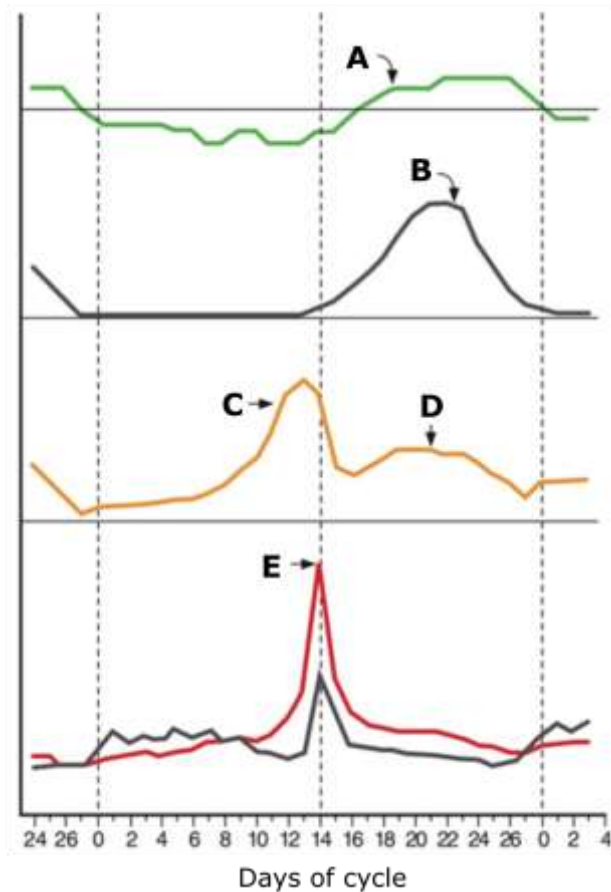


Figure 2:
Coronal T2-weighted
image of abdomen

- | | True | False |
|--|--------------------------|--------------------------|
| A. The figure 1 must be T1-weighted image due to higher signal intensity of white matter than grey matter. | <input type="checkbox"/> | <input type="checkbox"/> |
| B. If there is inflammation in a tissue the inflamed area would be of higher intensity in T2-weighted due to the resulting oedema. | <input type="checkbox"/> | <input type="checkbox"/> |
| C. the major secretions of the organ in figure 2 which is marked as A, are amylase and lipase. | <input type="checkbox"/> | <input type="checkbox"/> |
| D. In figure 2 the part B is shorter in herbivores than carnivore mammals. | <input type="checkbox"/> | <input type="checkbox"/> |

Q. 21 – Menstrual Cycle

The menstrual cycle is the regular natural change that occurs in the female reproductive system. In the ovary, where oogenesis take place, each cycle can be divided into three phases consisting of the follicular phase, ovulation and luteal phase. The menstrual cycle is controlled by hormones of hypothalamus-pituitary-ovary axis. The figure shows alternations in body temperature and hormonal changes during the menstrual cycle.



- A.** The increase shown at point A is caused by the effect of oestrogen on the anterior pituitary.
- B.** Curve B shows changes in progesterone level during menstrual cycle.
- C.** The source of the increase in concentrations indicated at point C and D are granulosa cells and corpus luteum, respectively.
- D.** Substance E is secreted by follicular cells.
- E.** The cause of the sudden increase shown at point E is positive feedback of oestrogen on the anterior pituitary and absence of progesterone.

True **False**

Q. 22 – Coombs Test

There are two clinical tests to detect some antibodies against erythrocytes (RBCs), direct coombs test and indirect coombs test.

During the direct coombs test a blood sample is taken from a person. RBCs are washed (removing the patient's own plasma) and then incubated with anti-human globulin, which attaches to all IgG antibodies. Coombs test is positive if agglutination reaction occurs.

In the indirect coombs test, serum is extracted from the blood sample taken from the person. Then, the serum gets incubated with RBCs of known antigenicity and is washed. Finally, anti-human globulin is added. If agglutination occurs, the indirect coombs test is positive.

- | | True | False |
|--|--------------------------|--------------------------|
| A. Direct coombs test will be positive only if autoantibodies are present. | <input type="checkbox"/> | <input type="checkbox"/> |
| B. If the result of indirect coombs test using serum of patient 1 and RBCs of patient 2 is positive, so we can use the patient 2 as a blood donor for patient 1. | <input type="checkbox"/> | <input type="checkbox"/> |
| C. Anti-human globulin specifically binds to the variable part of human antibodies. | <input type="checkbox"/> | <input type="checkbox"/> |
| D. In a positive indirect coombs test, antigen-antibody reaction happens <i>in vivo</i> . | <input type="checkbox"/> | <input type="checkbox"/> |

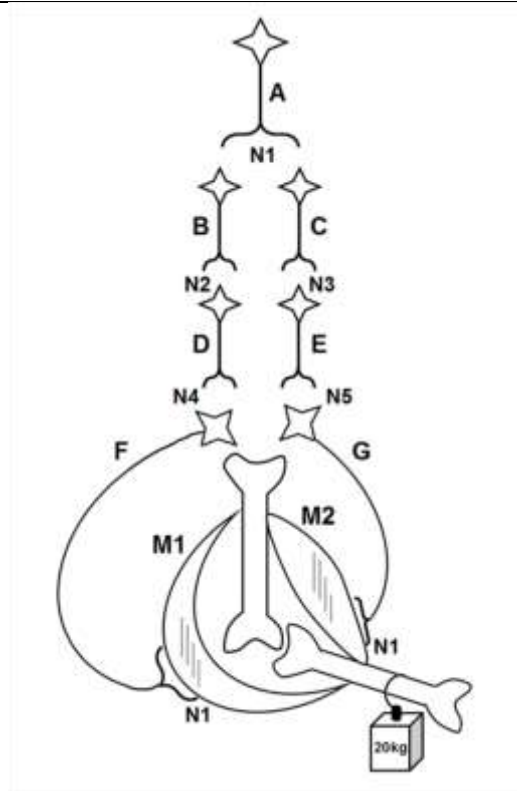
Q. 23 – Neural Network

The diagram below illustrates a neural pathway and the features of the associated neurotransmitters are described in the table.

Ions concentrations inside and outside of the cells are same as their physiological normal values in body and inhibition of an inhibitory neuron results in the stimulation of postsynaptic neuron.

“+” Symbol in table indicate the activation of the ion channels which increases the ion permeability across the membrane.

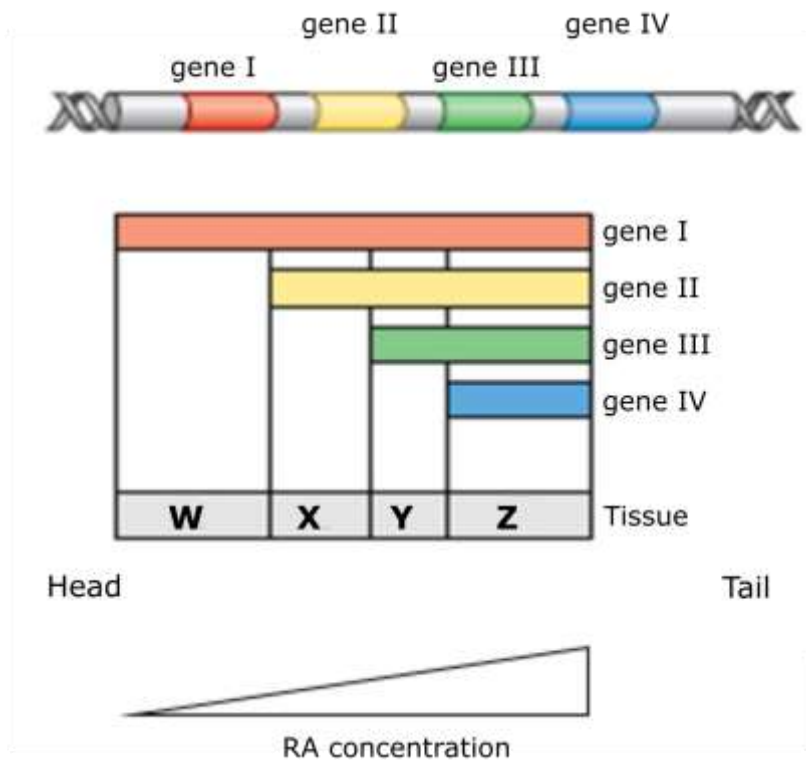
Neurotransmitter	Cl ⁻ Permeability	Na ⁺ Permeability	K ⁺ Permeability
N1		+	
N2	+		
N3			+
N4	+		
N5		+	



- | | True | False |
|---|--------------------------|--------------------------|
| A. The function of N1 neurotransmitter is same as acetylcholine. | <input type="checkbox"/> | <input type="checkbox"/> |
| B. Neuron G is not depolarized and neuron F is stimulated so muscle M1 contracts. | <input type="checkbox"/> | <input type="checkbox"/> |
| C. Neuron G gets depolarized as a result of Na ions influx. | <input type="checkbox"/> | <input type="checkbox"/> |
| D. Neuron F gets depolarized as a result of Cl ions efflux. | <input type="checkbox"/> | <input type="checkbox"/> |

Q. 24 – HOX Genes

Neural tube in the vertebrate embryos, lies the anterior-posterior (AP) axis and creates a variety of structures. There is a large body of evidence showing that AP patterning of the vertebrate embryos is controlled by *HOX* genes. Spatial and temporal expression patterns of *HOX* genes are controlled by factors usually present as gradients in the AP axis of embryos. One of these gradients is generated by retinoic acid (RA), a derivative of vitamin A, with a maximum concentration in the posterior region of the embryos (Figure below).



- A.** Overuse of vitamin A by pregnant women may cause abnormalities in the embryos.
- B.** In an embryo that has been affected by excessive amounts of RA in the early stages of embryogenesis, the forebrain may not form.
- C.** Loss of function of a *HOX* gene in the embryo may have the same effect as an excessive amount of RA.
- D.** In an embryo whose expression of RA nuclear receptors has been downregulated, the midbrain may develop similar to the forebrain.

True **False**

Q. 25 – Shell Coiling

In snail, the direction of cleavage, and therefore the snail shell coiling, is controlled by a single gene, in which the right-coiling allele, D, is dominant to the left-coiling allele, d. Below table shows the results of a set of mating experiment.

	Genotype	Phenotype
$DD_{\text{♀}} \times dd_{\text{♂}} \longrightarrow$	Dd	All right-coiling
$DD_{\text{♂}} \times dd_{\text{♀}} \longrightarrow$	Dd	All left-coiling
$Dd \times Dd \longrightarrow$	1DD:2Dd:1dd	All right-coiling

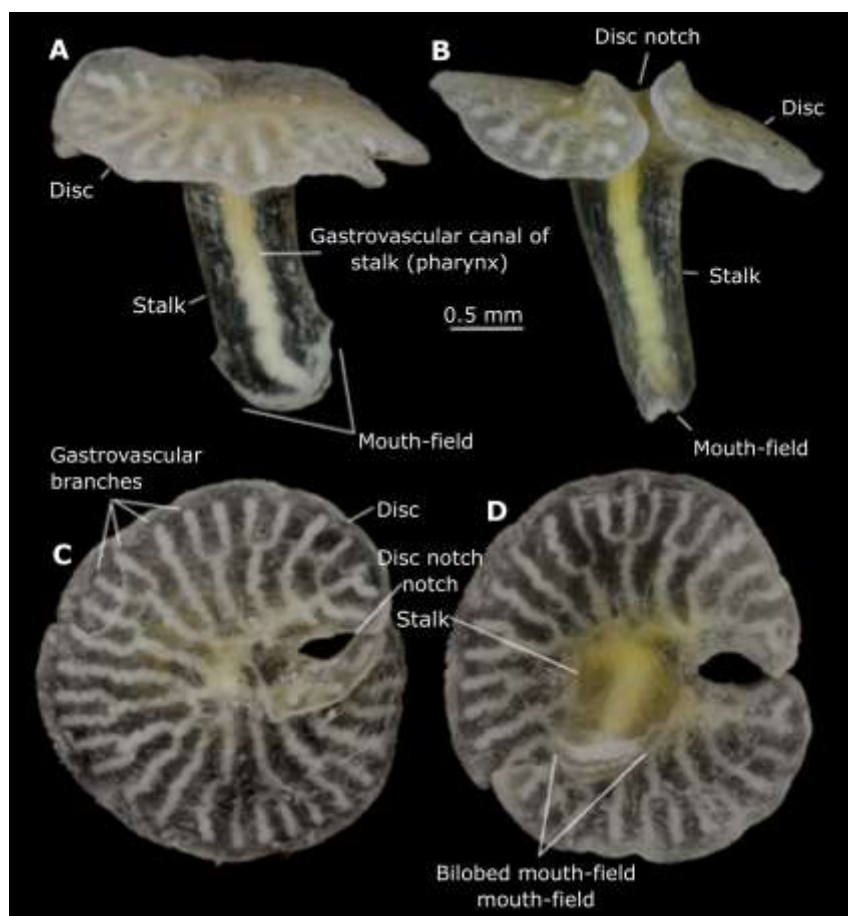
- | | True | False |
|---|--------------------------|--------------------------|
| A. The direction of cleavage is determined by the genotype of the developing snail. | <input type="checkbox"/> | <input type="checkbox"/> |
| B. If the egg cytoplasm of a recessive homozygous right-coiling mother is injected into the eggs of the “dd” mother, the resulting embryos coil to the left. | <input type="checkbox"/> | <input type="checkbox"/> |
| C. Injection of the egg cytoplasm from a heterozygous left-coiling mother into the eggs of the right coiling heterozygous mother, does not affect the right-coiling in the embryos. | <input type="checkbox"/> | <input type="checkbox"/> |
| D. “DD” or “Dd” mothers place a coiling determinant factor inside the egg cytoplasm. | <input type="checkbox"/> | <input type="checkbox"/> |

Q. 26 – *Dendrogramma*

Dendrogramma is a new animal species which has been collected at 400 and 1000 metres on the Australian continental slope off eastern Bass Strait and Tasmania during a cruise in 1986 and described as a new taxon in 2016. The new taxon is multicellular (metazoan), non-bilateralian, apparently diploblastic with a dense mesoglea between an outer epidermis and an inner gastrodermis.

This animal is composed of a body divided into a stalk with a mouth opening terminally, and a flattened disc. The mouth is set in a specialized, lobed epidermis field, leading into a gastrodermis-lined gastrovascular canal (pharynx) in the stalk which aborally branches dichotomously into numerous radiating canals in the disc. We can state with considerable certainty that the organisms lack cnidocytes, tentacles, marginal pore openings for the radiating canals, ring canal, sense organs in the form of statocysts or the rhopalia, or colloblasts, ctenes, or an apical organ.

No cilia have been located. They have simple mouth opening with specialized lobes secreting mucus.

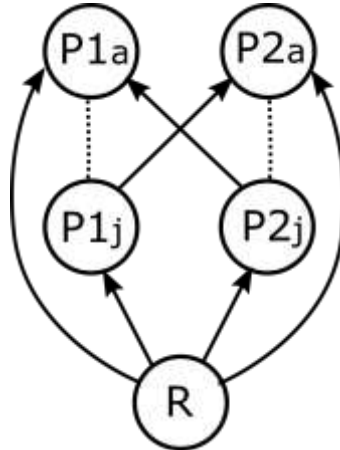


- A.** According to the characteristics of *Dendrogramma* it could be placed in Cnidaria.
- B.** It seems likely that *Dendrogramma* feed on micro-organisms.
- C.** Lack of statocysts and rhopalia shows that this taxon does not have nervous system.
- D.** Most likely *Dendrogramma* could have Dinoflagellate symbionts such as *Symbiodinium*.

True	False
<input type="checkbox"/>	<input type="checkbox"/>
<input type="checkbox"/>	<input type="checkbox"/>
<input type="checkbox"/>	<input type="checkbox"/>
<input type="checkbox"/>	<input type="checkbox"/>

Q. 27 – Intraguild Predation

Intraguild predation is the killing and sometimes eating of potential competitors. Reciprocal intraguild predation with size structure, is one type of intraguild predation where both consumers feed on each other's juveniles. In this case, P1 has piercing-sucking type mouthparts, and P2 has chewing type mouthparts. In the figure below "R" represents resource, "P" represents (reciprocal) intraguild predator, "j" represents juveniles and "a" represents adults.

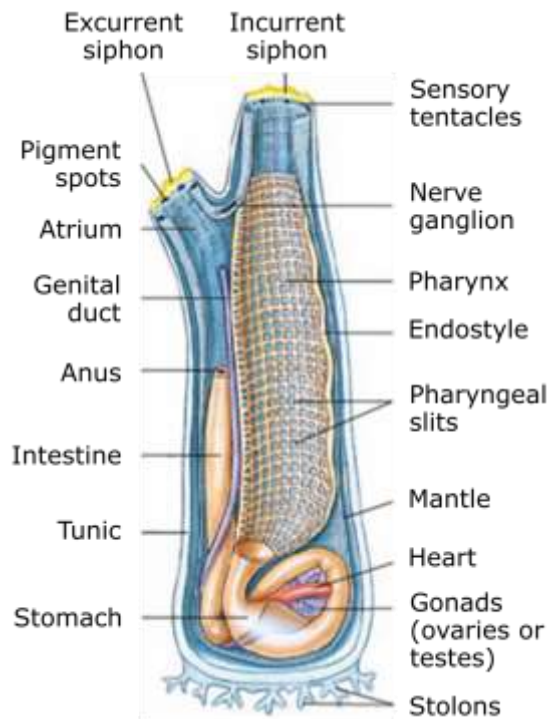


- A.** If P1j population increases, then P2a will produce more eggs.
- B.** If P2j population decreases, then P2a population will increase in next generation.
- C.** If R increases, then P2a doesn't feed on P1j.
- D.** If R decreases, then P2a population will increase in next generation.

True **False**

Q. 28 – Tunicate Morphology

Five distinctive characteristics that, taken together, set chordates apart from all other phyla are notochord, dorsal tubular nerve cord, pharyngeal pouches or slits, an iodine secreting organ (endostyle), and post-anal tail. These characteristics are always found at some embryonic stage, although they may be altered or may disappear in later stages of the life cycle. Tunicates belong to Deuterostomia group of Metazoa and are found in all seas from near shoreline to great depths. Most are sessile as adults, although some are free-living. The name “tunicate” refers to the usually tough and non-living tunic that surrounds the animal and contains cellulose-like components. As adults, tunicates are highly specialized chordates, for in most species only the larval form, which resembles a microscopic tadpole, bears all the chordate hallmarks. Tadpole undergoes metamorphosis and changes its morphology and anatomy.

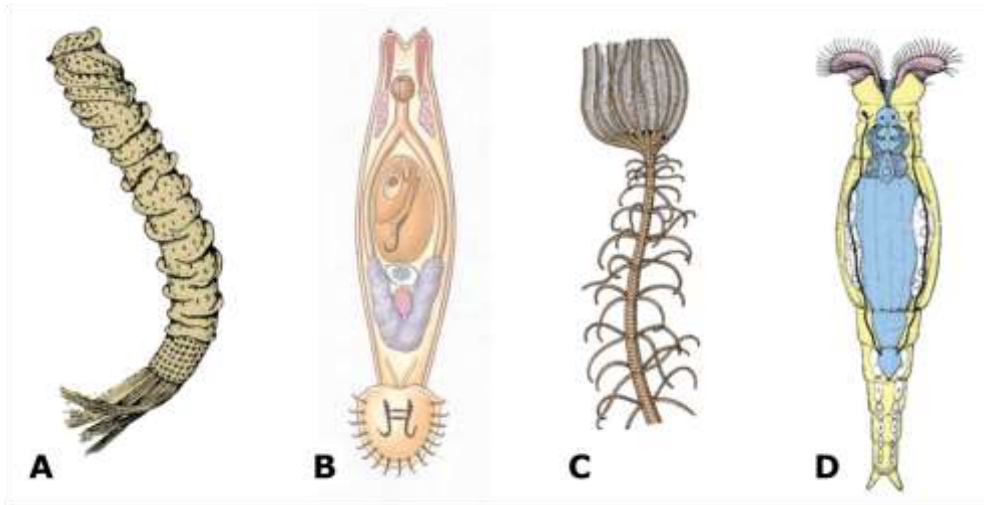


Structure of a common tunicate, *Ciona* sp.

- | | True | False |
|--|--------------------------|--------------------------|
| A. Adult of tunicates shows two shared derived characters, which are present in all chordates. | <input type="checkbox"/> | <input type="checkbox"/> |
| B. Main pathway for seawater is: incurrent siphon, gut, anus, atrium and excurrent siphon. | <input type="checkbox"/> | <input type="checkbox"/> |
| C. In <i>Ciona</i> , the notochord is homologous to backbone of vertebrates. | <input type="checkbox"/> | <input type="checkbox"/> |
| D. <i>Ciona</i> belongs to the coelomate vertebrate group and coelom forms from fusion of enterocoelous pouches. | <input type="checkbox"/> | <input type="checkbox"/> |

Q. 29 – Metazoa Taxonomy

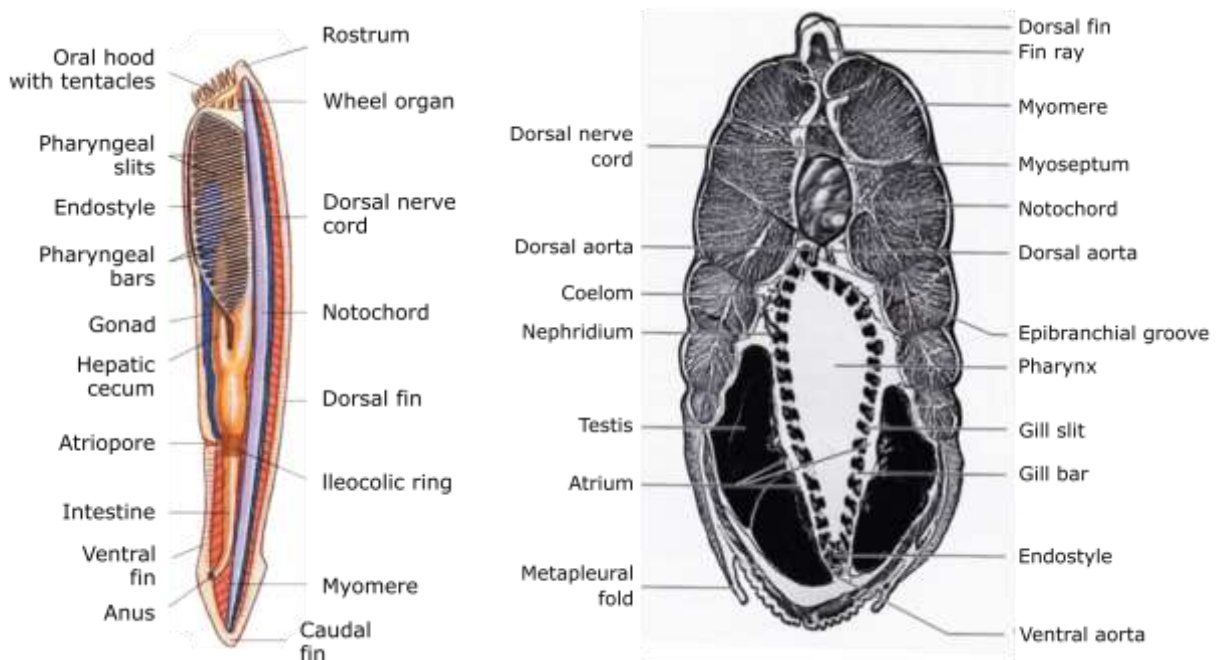
You are given four figures referring to typical representatives of four major phyla of animals.



- | | True | False |
|--|--------------------------|--------------------------|
| A. Organism A belongs to a taxon characterized by unique aquiferous system, radial or no symmetry and lack of tissue and organ systems. | <input type="checkbox"/> | <input type="checkbox"/> |
| B. Organism B belongs to a taxon characterized by bilateral symmetry, lack of coelom, protonephridia and ladder-like nervous system. | <input type="checkbox"/> | <input type="checkbox"/> |
| C. Organism C belongs to a taxon characterized by entocoelic development, pentaradial symmetry and metamorphosis. | <input type="checkbox"/> | <input type="checkbox"/> |
| D. Organism D belongs to a taxon characterized by radial symmetry, hydrostatic skeleton and schizocoelic development. | <input type="checkbox"/> | <input type="checkbox"/> |

Q. 30 – Amphioxus Morphology

Amphioxus (lancelet) is a marine slender, laterally compressed and translucent filter-feeder deutrostome that inhabits the sandy bottoms of coastal waters around the world. Sexes are separate, gonads are located in the atrial cavity and there are no ducts. The closed circulatory system of this fish-like animals, is complex for such a simple chordate. The flow pattern is remarkably similar to that of primitive vertebrates. The colourless blood is pumped forward in the ventral aorta by peristaltic-like contractions of the vessel wall only, then passes upward through branchial arteries (aortic arches) in the pharyngeal bars to paired dorsal aortas which join to become a single dorsal aorta. From here the blood is distributed to the body tissues by microcirculation and then is collected in veins, which return it to the ventral aorta.



- | | True | False |
|--|--------------------------|--------------------------|
| A. The blood is circulated from anterior to posterior dorsally and from posterior to anterior ventrally. | <input type="checkbox"/> | <input type="checkbox"/> |
| B. The heart consists of a sinuous venous, a cardiac atrium, and a ventricle located ventrally and carries low oxygen blood. | <input type="checkbox"/> | <input type="checkbox"/> |
| C. It differs from vertebrates in having numerous pharyngeal slits that are not open outside directly but acts as a trapping structure to collect small-suspended particles. | <input type="checkbox"/> | <input type="checkbox"/> |
| D. Sperms are released into the atrial cavity, and then pass out via genital pore and atriopore to the outside where fertilization occurs. | <input type="checkbox"/> | <input type="checkbox"/> |

Q. 31 – Electrocardiography

Electrocardiography is a method to study the electrical activity of the heart (ECG). In addition to P, QRS and T waves, there are segments and intervals which are defined to show a specific period of time in a cardiac cycle. A variety of different factors like concentration of electrolytes, drugs and temperature could have an effect on waves and intervals of ECG. A group of researchers have studied the effect of body temperature on QT and RR interval in electrocardiogram of beagle dogs. The result of their study is demonstrated in the figures.

Note that RR interval is the time between two consecutive R waves and QT interval is the exact time before start of Q wave till the end of the next T wave.

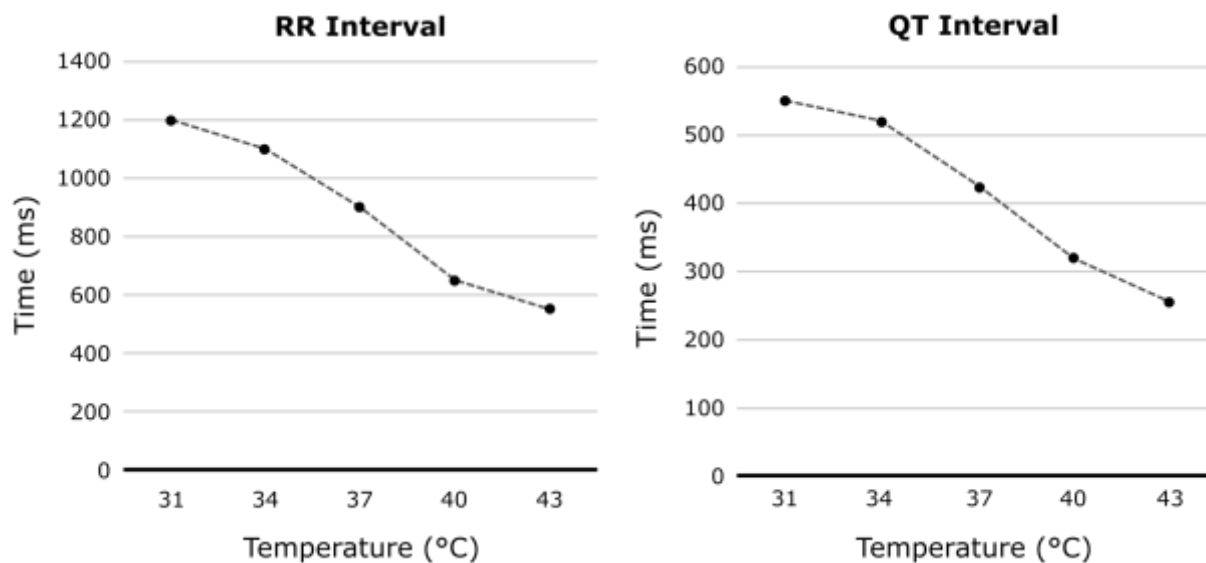


Figure (left) Relation between RR Interval and body temperature. (right) Relation between QT Interval and body temperature.

Given that QT interval gets shortened by the shortening of the RR interval, a formula (given below) has been approved to calculate a corrected QT interval (QTc) to allow the comparison of QT interval over time at different heart rates.

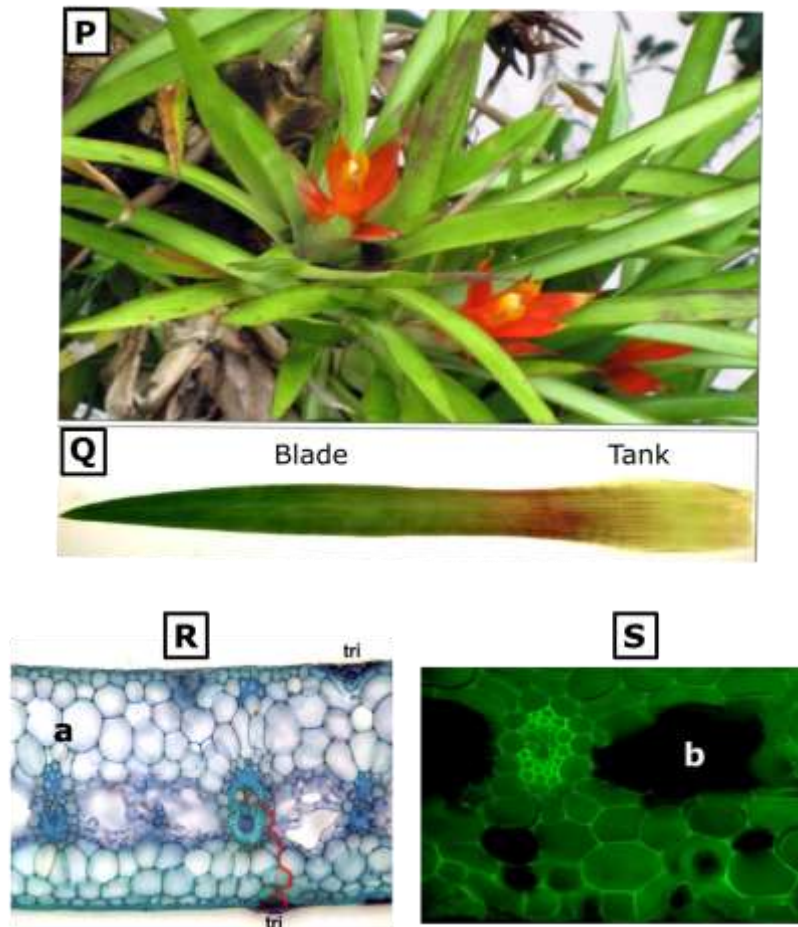
$$\text{Hodges formula: } \text{QTC} = \text{QT} + 1.75 (\text{heart rate} - 60)$$

- | | True | False |
|--|--------------------------|--------------------------|
| A. Body temperature does not have any effect on heart rate. | <input type="checkbox"/> | <input type="checkbox"/> |
| B. Independent of changes of heart rate, QT interval is shortened by rise of body temperature. | <input type="checkbox"/> | <input type="checkbox"/> |
| C. Hypocalcaemia will shorten the QTc interval. | <input type="checkbox"/> | <input type="checkbox"/> |
| D. In higher body temperature, end diastolic volume of ventricles is increased. | <input type="checkbox"/> | <input type="checkbox"/> |

Q. 32 – Bromeliad Morphology

Some plants in the Bromeliaceae essentially lack stems and absorptive roots. They take up water from reservoirs known as “tanks” that are formed by overlaps of bases of different leaves (Fig. P–Q). All Bromeliads have profuse trichome coatings on both sides of their leaves. The coatings consist of tiny sliver white cells that are able to take up moisture and nutrients and transfer these into the plant.

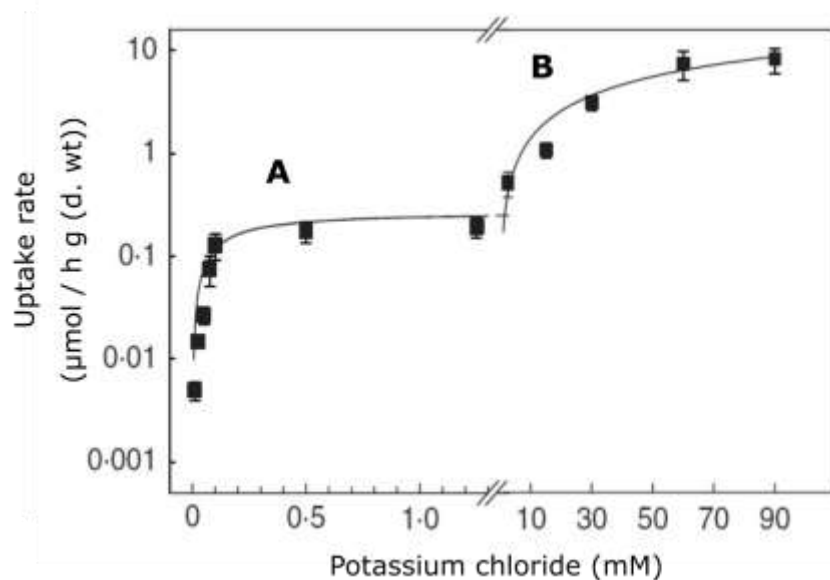
Morphology and anatomy of leaf of a bromeliad is shown. The leaf was cut at the base of the tank region, sealed, and immersed in aqueous solution of a fluorescent dye, for 2 h. Cross-sections were made from the blade (Fig. R) and tank (Fig. S) before and after staining, respectively. Red line indicates pathway for water between vein and trichome (tri).



- | | True | False |
|---|--------------------------|--------------------------|
| A. “a” in Figure R denotes aerenchyma | <input type="checkbox"/> | <input type="checkbox"/> |
| B. “b” in Figure S denotes hydrenchyma (aquatic parenchymal cells) | <input type="checkbox"/> | <input type="checkbox"/> |
| C. The leaf anatomy suggests a C4 or CAM photosynthetic type | <input type="checkbox"/> | <input type="checkbox"/> |
| D. Red line indicates pathway for water between vein and trichome on the upper side of leaf (adaxial) | <input type="checkbox"/> | <input type="checkbox"/> |

Q. 33 – Potassium Acquisition

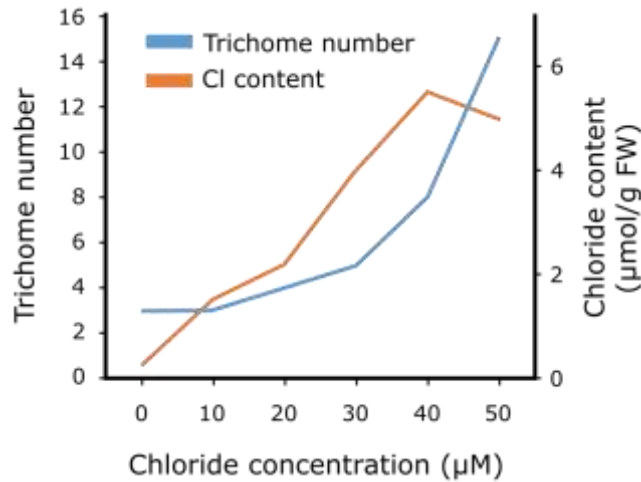
Physiological studies have been accomplished on the adaptations of bromeliad plants to nutrient acquisition and plant utilization of potassium. The Figure shows biphasic kinetics of potassium uptake by foliar trichomes of a tank bromeliad plant in the presence of 0.01–90 mM substrate. Uptake rates were calculated during the first 1–2 h of the experiment. The obtained results suggested that there were two transporter systems, and their Michaelis–Menten constants (K_m) were calculated to be $41.3 \pm 8.7 \mu\text{M}$ and $56.5 \pm 13.7 \text{ mM}$.



- | | True | False |
|---|--------------------------|--------------------------|
| A. The low affinity system accumulated K^+ slower than the high affinity system | <input type="checkbox"/> | <input type="checkbox"/> |
| B. K_m of 56.5 mM belongs to B transporter system | <input type="checkbox"/> | <input type="checkbox"/> |
| C. Applying ATPase inhibitor compounds inhibits B transporters | <input type="checkbox"/> | <input type="checkbox"/> |
| D. B transporters are blocked more by potassium channel blockers, as compared to A transporters | <input type="checkbox"/> | <input type="checkbox"/> |

Q. 34 – Chlorine Uptake

The relationship between trichome density on leaves and ion uptake was plotted from a bromeliad plants treated with different concentrations of chloride during 1 week.



The relationship between chloride supply, trichome number and chlorine uptake.

- | | True | False |
|---|--------------------------|--------------------------|
| A. The results suggest that chloride is only absorbed by bromeliad trichoms. | <input type="checkbox"/> | <input type="checkbox"/> |
| B. Induction of trichomes occurs at any increase in concentration of exogenously applied chloride. | <input type="checkbox"/> | <input type="checkbox"/> |
| C. There is an exponential relationship between the chloride concentration and absorbed chloride by leaf trichomes. | <input type="checkbox"/> | <input type="checkbox"/> |
| D. Chloride is actively excluded or secreted above 40 μM concentration. | <input type="checkbox"/> | <input type="checkbox"/> |

Q. 35 – Plant Taxonomy

In a scientific excursion the students found four plant specimens that they had never seen before. They studied the plant organs carefully and made a few sections from them to look for the plants transport systems. The following table was completed based on their observation.

Plant number	Companion cell	Sieve cell	Sieve tube cell	Tracheid	Vessel elements	Pollen
1	+	-	+	+	+	+
2	-	+	-	+	-	+
3	+	-	+	+	+	-
4	-	+	-	+	-	-

- | | True | False |
|--|--------------------------|--------------------------|
| A. Plant 1 has seeds with more than two cotyledons. | <input type="checkbox"/> | <input type="checkbox"/> |
| B. Plant 2 has winged pollen grain and double fertilization. | <input type="checkbox"/> | <input type="checkbox"/> |
| C. Plants 3 and 1 have smaller female gametophyte as compared to plants 2 and 4. | <input type="checkbox"/> | <input type="checkbox"/> |
| D. Plant 3 does not belong to the flowering plants, because it does not have pollen grain. | <input type="checkbox"/> | <input type="checkbox"/> |

Q. 36 – Plant Phylogenetics

The plant genus X contains 6 species (*X. messa*, *X. obnoxia*, *X. beatifica*, *X. confusa*, *X. foetida*, *X. nerda*). All of them share many character states that distinguish this genus from all closely related genera. The species differ from each other, however, as described below. All species in the sister genus, Y, are vining plants with palmately compound, alternate leaves, sweet-smelling flowers with pink, free petals and 10 stamens, and drupes.

X. messa: Plant upright, stems glabrous; leaves opposite, palmately compound; petals purple, free; stamens 5; flowers sweet-smelling; fruit a berry

X. obnoxia: Plant vining, stems glabrous; leaves opposite, simple; petals red, free; stamens 10; flowers with a rotten meat smell; fruit a berry

X. beatifica: Plant upright, stems glabrous; leaves opposite, palmately compound; petals pink, connate; stamens 5; flowers sweet-smelling; fruit a berry

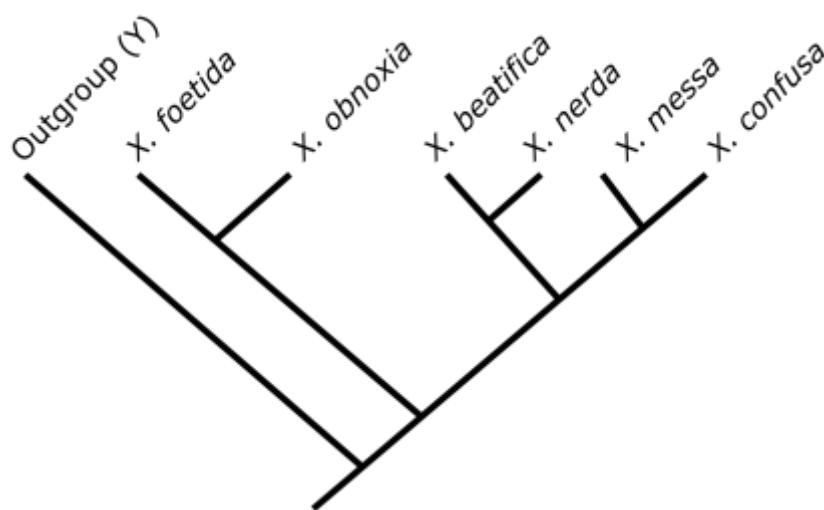
X. confusa: Plant upright, stems glabrous; leaves opposite, simple; petals purple, free; stamens 5; flowers sweet-smelling; fruit a berry

X. foetida: Plant vining, stems hispid; leaves opposite, palmately compound; petals red, free; stamens 10; flowers with a rotten meat smell; fruit a berry

X. nerda: Plant upright, stems glabrous; leaves opposite, palmately compound; petals pink, connate; stamens 4; flowers sweet-smelling; fruit a berry

The data matrix, in which characters are coded according to whether character states are plesiomorphic (0) or apomorphic (1, 2) was presented in the following table. The most parsimonious cladogram was constructed from the data matrix.

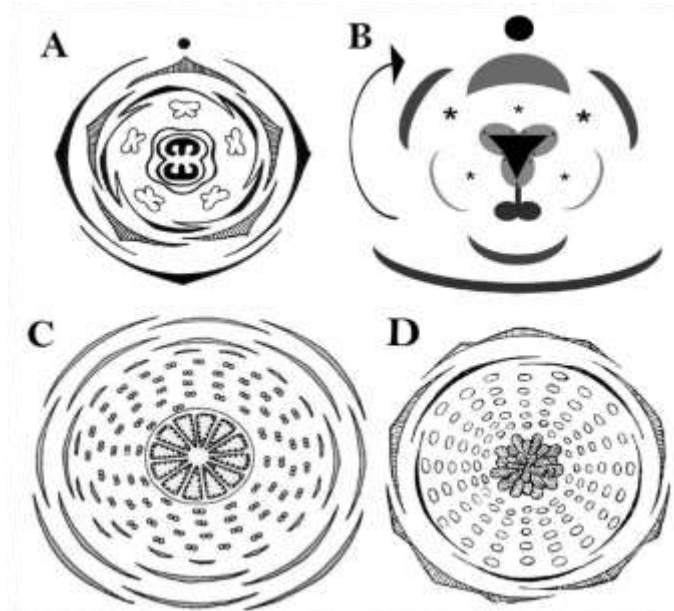
	Habit	Stem hairs	Leaf position	Leaf structure	Petal colour	Petal fusion	Stamen number	Flower odour	Fruit type
<i>X. messa</i>	1	0	1	0	2	0	1	0	1
<i>X. obnoxia</i>	0	0	1	1	1	0	0	1	1
<i>X. beatifica</i>	1	0	1	0	0	1	1	0	1
<i>X. confusa</i>	1	0	1	1	2	0	1	0	1
<i>X. foetida</i>	0	1	1	0	1	0	0	1	1
<i>X. nerda</i>	1	0	1	0	0	1	2	0	1
Outgroup (Y)	0	0	0	0	0	0	0	0	0



- | | True | False |
|---|--------------------------|--------------------------|
| A. Fruit as a berry and leaves opposite support the monophyly of the genus <i>X</i> . | <input type="checkbox"/> | <input type="checkbox"/> |
| B. <i>X. obnoxia</i> , <i>X. beatifica</i> and <i>X. nerda</i> form a monophyletic group. | <input type="checkbox"/> | <input type="checkbox"/> |
| C. Hispid stems and 4 stamens are autapomorphic (unique) for <i>X. foetida</i> and <i>X. nerda</i> , respectively. | <input type="checkbox"/> | <input type="checkbox"/> |
| D. Simple leaves in <i>X. obnoxia</i> and <i>X. confuse</i> appear to have evolved independently. | <input type="checkbox"/> | <input type="checkbox"/> |

Q. 37 – Floral Diagrams

The flowering plants show great diversity in their flower structure reflecting evolutionary changes in course of time. One method to illustrate the flower morphology is the usage of floral diagrams implementing various shapes and symbols to show the structure as exact as possible.

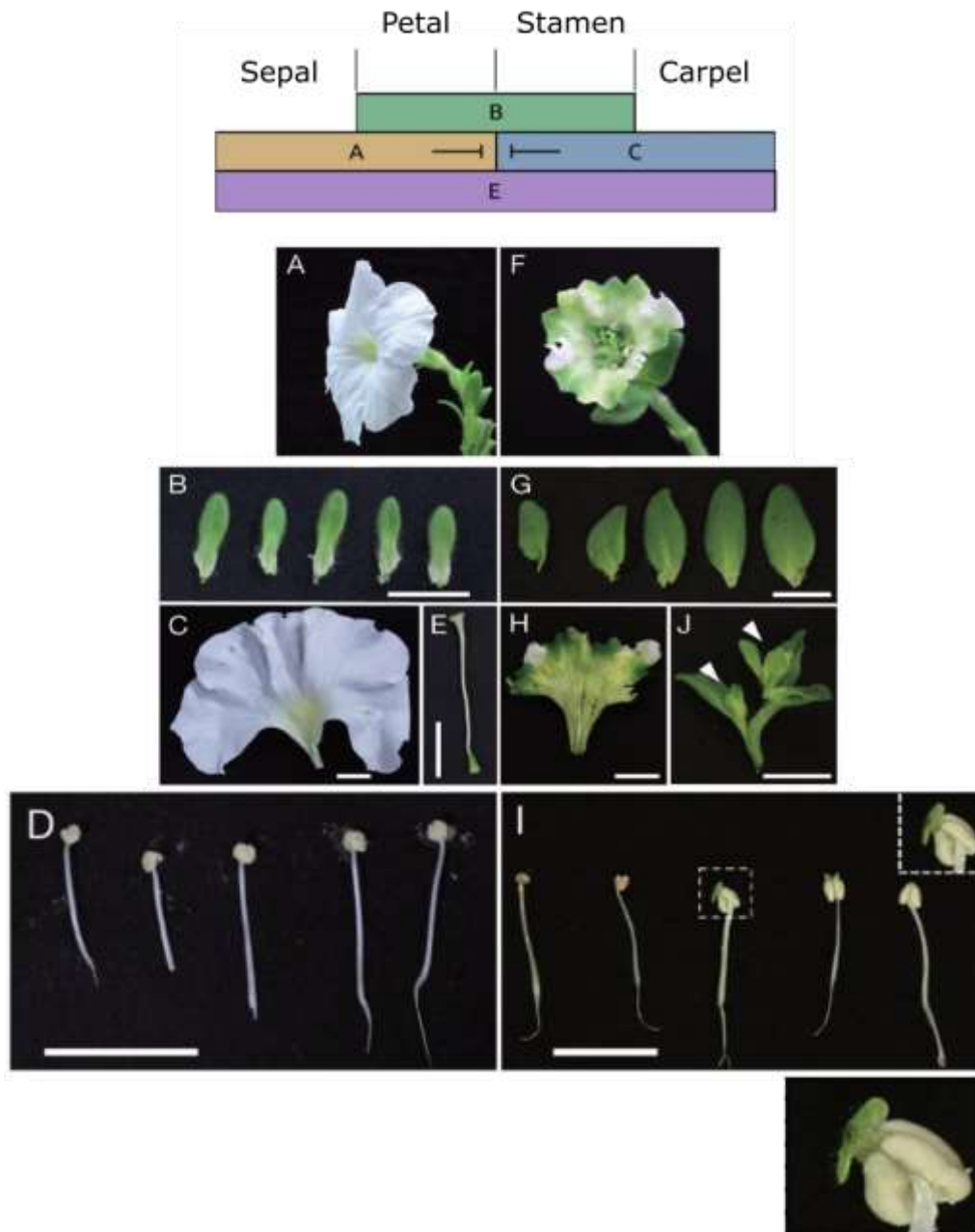


- | | True | False |
|--|--------------------------|--------------------------|
| A. Diagram A can represent a basal herbaceous dicot. | <input type="checkbox"/> | <input type="checkbox"/> |
| B. Diagram B may represent a species from the family Orchidaceae with 2 sterile stamens. | <input type="checkbox"/> | <input type="checkbox"/> |
| C. The most primitive flower among the illustrated diagrams in this task is C. | <input type="checkbox"/> | <input type="checkbox"/> |
| D. Diagram D belongs to a same family as C. | <input type="checkbox"/> | <input type="checkbox"/> |
| E. The perianth in diagram B is composed of 3 whorls. | <input type="checkbox"/> | <input type="checkbox"/> |

Q. 38 – ABCE Model of Flower Development

The diagram below illustrates the ABCE model of flower development, in which the identity structure of floral organs of eudicots is regulated by floral homeotic genes divided into ABCE-classes, based on function: A- and E-class genes specify sepal identity; A-, B-, and E-class genes petal identity; B-, C-, and E-class genes stamen identity; and C- and E-class genes carpel identity.

ABCE-class MADS domain transcription factors (MTFs) are key regulators of floral organ development in eudicots. Aberrant expression of these genes can result in abnormal floral traits, such as phyllody. Certain plant pathogenic bacteria could trigger phyllody in particular species, such as *Petunia*, which is shown in the figures below.

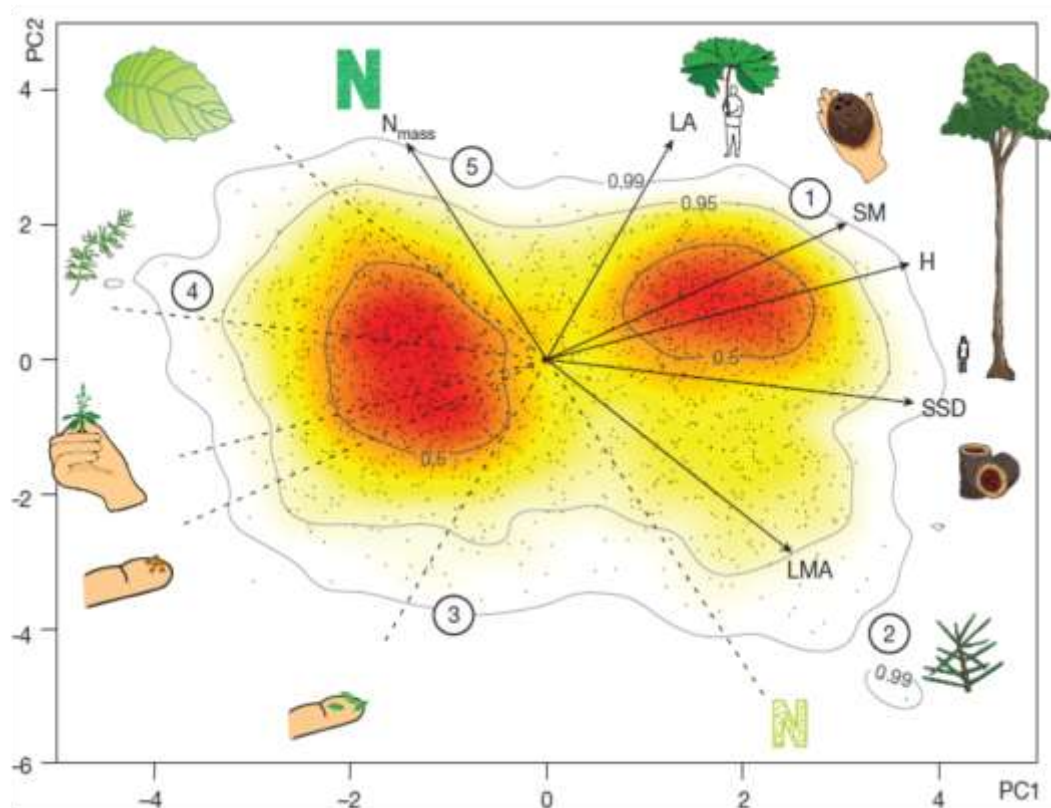


A–E are parts of a control flower and F–I are parts of a bacteria-treated flower. The same parts of the flowers are shown in B and G, C and H, D and I, and E and J.

- | | True | False |
|--|--------------------------|--------------------------|
| A. The bacteria caused perianth fusion of Petunia. | <input type="checkbox"/> | <input type="checkbox"/> |
| B. The bacteria caused the expression of the protein coded by Gene E. | <input type="checkbox"/> | <input type="checkbox"/> |
| C. The bacteria decreased the frequency of moths landing on the flower. | <input type="checkbox"/> | <input type="checkbox"/> |
| D. The bacteria treatment proved that the flower reproductive parts are leaf modifications. | <input type="checkbox"/> | <input type="checkbox"/> |

Q. 39 – Trait Variation among Vascular Plants

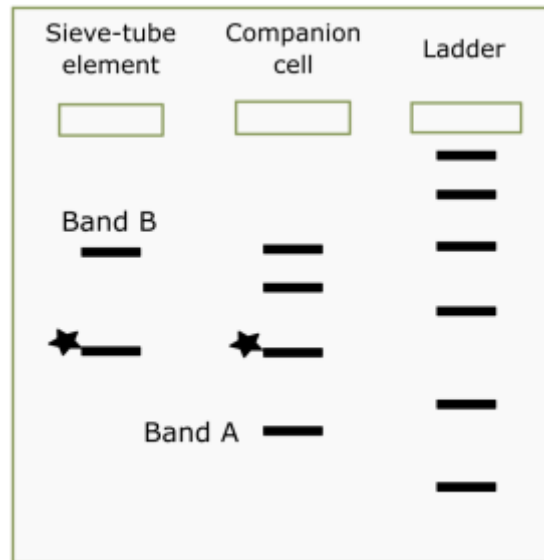
During last 500 million years, a great amount of trait variation has been created in land plants in the course of evolution. However, there are some constraints over the possible combinations of traits which indicate evolutionary limitations and trade-offs. To investigate trait combinations in more than 46,000 extant vascular plants, a Principal component analysis was conducted (Díaz *et al.* 2016). Principal component analysis (PCA) is a statistical procedure converts a set of observations of possibly correlated variables into a set of values of linearly uncorrelated variables called principal components. Figure 1-a shows distribution of investigated vascular plants (including angiosperms, gymnosperms and pteridophytes) in a space conducted by the PCA analysis. Each trait changes along its corresponding axis in this space. Areas with high density of points indicate functional hotspots. There are two major hotspots corresponding to woody and non-woody plants (LA: leaf area, SM: diaspore (fruit or spore) mass, H: plant height, SSD: stem specific density, LMA: leaf mass per area, N_{mass} : leaf nitrogen content per mass.)



- | | True | False |
|---|--------------------------|--------------------------|
| A. Woody plants tend to have higher N_{mass} than non-woody plants. | <input type="checkbox"/> | <input type="checkbox"/> |
| B. Plants inhabiting temperate grasslands tend to place near points 4 and 5. | <input type="checkbox"/> | <input type="checkbox"/> |
| C. Dominant plants of boreal forests are mostly to locate near point 1. | <input type="checkbox"/> | <input type="checkbox"/> |
| D. Plants inhabiting tropical forests tend to have higher LMA than plants inhabiting temperate forests. | <input type="checkbox"/> | <input type="checkbox"/> |
| E. N_{mass} correlates with leaf lifespan negatively. | <input type="checkbox"/> | <input type="checkbox"/> |

Q. 40 – Sieve-Tubes

Plants conduct sugars and other substances throughout their body by means of phloem. Phloem is a compound tissue, including different cell types (e.g. sieve-tubes elements (in angiosperms), companion cells and parenchymal cells.). In a study, DNA genomic samples prepared from sieve-tubes and companion cells of an angiosperm and investigated for DNA corresponding to X. Gene-specific primers were used to amplify gene X among whole genome of cells by PCR.

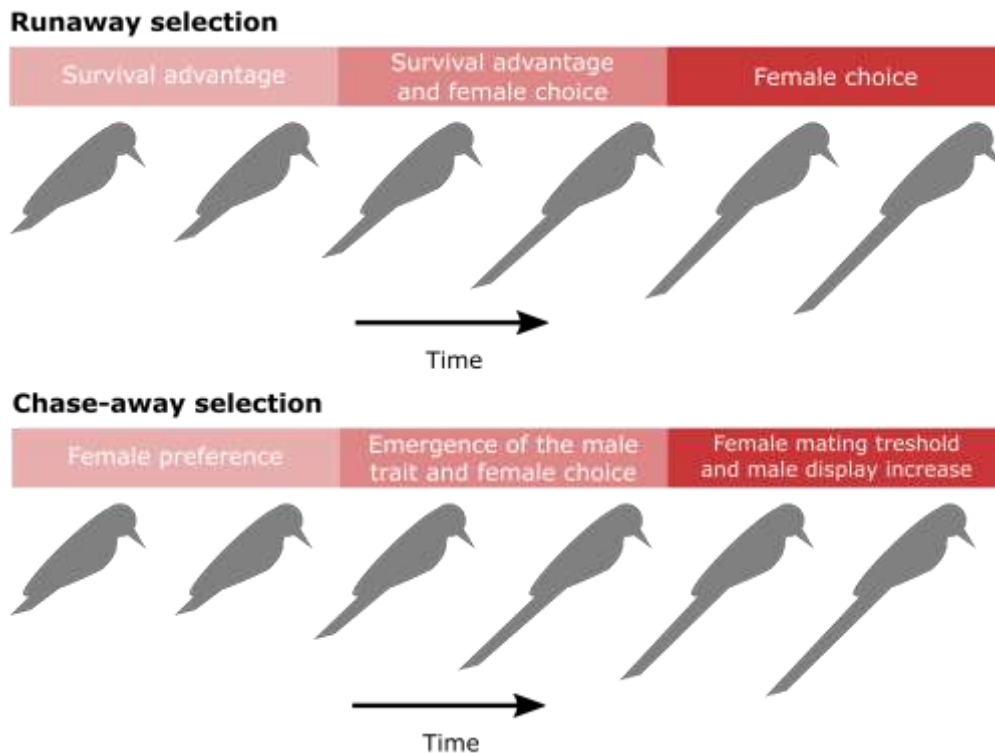


Note: Each band represents a unique DNA molecule, asterisks denotes bands corresponding to functional genes.

- | | True | False |
|--|--------------------------|--------------------------|
| A. Results of sieve-tube element genome analysis suggest that the plant is heterozygote in the gene X. | <input type="checkbox"/> | <input type="checkbox"/> |
| B. The results obtained for the sieve-tube cells can be explained by gene X being present both in the mitochondrial and chloroplast DNA. | <input type="checkbox"/> | <input type="checkbox"/> |
| C. Band A most likely corresponds to an organelle-related DNA sequences in the nuclear genome. | <input type="checkbox"/> | <input type="checkbox"/> |
| D. Band B most likely corresponds to a pseudogene in nuclear genome. | <input type="checkbox"/> | <input type="checkbox"/> |

Q. 41 – Evolution of Sexual Traits

Evolution of sexual traits such as horn size, tail feathers and extreme coloration can be determined by sexual selection theory. According to the sexual selection theory male with such attributes gain an advantage over other males to acquire mate. Two processes have been proposed to account for exaggerated traits as the result of sexual selection (figure below).



Runaway selection: Imagine some males with traits (such as tail length) with the higher survival rates than other males in same population. In this ancestral population, some females start to prefer these males. Their offspring will inherit both of these traits (higher tail length in males and female choice for such traits in males). This pattern generates a runaway process until the male trait becomes so exaggerated that it becomes selected against by natural selection.

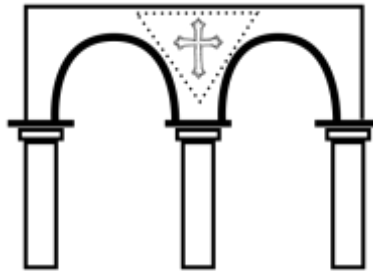
Chase-away selection: A mutation in males provides them with a novel trait that becomes sexually attractive to the females, and changes female mate choice in favour of such novel trait. Males with this mutation can easily mate with the females, while they don't offer any material or genetic benefit to the females. When such choice becomes disadvantageous for the females, the females' threshold increases against such a trait. Males with more extreme forms trait will again attract the females and this process will continue until natural selection selects against this exaggerated trait.

- | | True | False |
|--|--------------------------|--------------------------|
| A. In chase away selection, female choice correlates with male attributes that increase female fitness. | <input type="checkbox"/> | <input type="checkbox"/> |
| B. Extreme traits will evolve in males according to the runaway selection and will decrease male life expectancy. | <input type="checkbox"/> | <input type="checkbox"/> |
| C. Male attributes that become extreme because of chase-away selection will reduce male life expectancy. | <input type="checkbox"/> | <input type="checkbox"/> |
| D. Sensory bias is the primary requirement for chase-away selection to be evolved, but is not necessary for runaway selection. | <input type="checkbox"/> | <input type="checkbox"/> |

Q. 42 – Adaptations

Basilica of St Mark in Venice is an architectural marvel built in the 11th century CE. When examining the architecture, it is hard to avoid the spandrels in the corners of the ceiling, like the one in the figure (the triangular shape delineated by the dotted lines).

Gould & Lewontin (1979) argue that these spandrels are the result of simple geometric constraints one encounters when trying to hold a dome with column and arches. If we were to use the tools of evolutionary biology we would at first consider the spandrels as “adaptations” for the purpose of having the decorations, but in fact they are non-adaptive features, and we cannot count them as adaptations.



- | | True | False |
|---|--------------------------|--------------------------|
| A. If the feather characteristic of birds first evolved in dinosaurs for the purpose of thermal regulation, that feather is similar to spandrels. | <input type="checkbox"/> | <input type="checkbox"/> |
| B. When investigating the evolution of small regulatory RNAs (where the phenotype is closely tied to the genotype), biologists should not presume adaptation to avoid mistaking “spandrels” for true adaptations. | <input type="checkbox"/> | <input type="checkbox"/> |
| C. Biological “spandrels” are more common in species with historically high population size. | <input type="checkbox"/> | <input type="checkbox"/> |
| D. The evolution of big brain in humans would be a biological spandrel if its evolutionary trajectory is constrained by developmental process in primates. | <input type="checkbox"/> | <input type="checkbox"/> |

Q. 43 – Godfrey-Smith Model

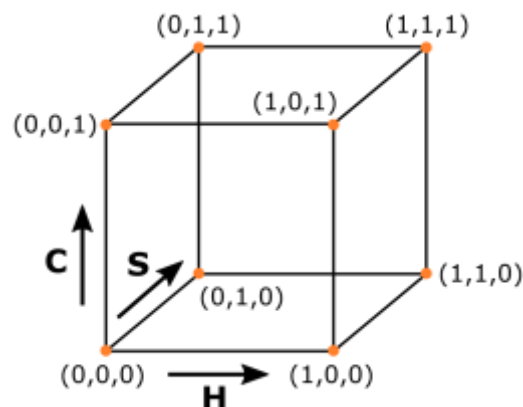
Peter Godfrey-Smith (2009) describes a parameter space in which a population can evolve using three parameters:

H: Fidelity of heredity

S: Dependence of reproductive differences on genetic differences

C: Continuity (when C is maximum, adding beneficial mutations to a genome results in the proportional betterment of the genotype. When C is zero, the effect of each mutation is entirely dependent on all the other loci)

We can imagine this space as cube (described by Peter Godfrey-Smith as A Darwinian space), as seen in the figure.



- A.** Accumulation of excessive mutations can result in the extinction of a population. (0,1,1) in the Darwinian space describes this situation.
- B.** In the absence of selection, a population of organisms resides at (1,0,0).
- C.** If your attempts at optimizing a bacteria species to consume glucose almost always results in sub-optimized populations, you are exploring the space close to (1,0,1).
- D.** A somatic cell in the human body can reside at (0,1,1) (Here, heredity is defined for the human and not the cell.).

True **False**

Q. 44 – Mutation Rates

The lack of advanced molecular biology methods, such as DNA sequencing or site-directed mutagenesis, did not stop the pioneers of evolution from asking difficult questions concerning the fundamental aspects of biological systems. J. B. S. Haldane's attempt to calculate the mutation rate in the 1930s is an illuminating example.

With no direct genetic evidence, he focused on men living in London and hemophilia A, an X-linked recessive disorder. Assuming that men with this disorder do not reproduce, his calculations show that the mutation rate is three times the frequency of men with this disorder in London. His estimate of mutation per generation per locus is not that different from the more recent estimates for many genes.

- | | True | False |
|--|--------------------------|--------------------------|
| A. The purported relationship between mutation rate and frequency of that mutation is only limited to populations that have reached mutation selection equilibrium. | <input type="checkbox"/> | <input type="checkbox"/> |
| B. For a recessive autosomal disorder that results in sterility, one would expect mutation rate to be equal to six times the frequency of that disorder in a population. | <input type="checkbox"/> | <input type="checkbox"/> |
| C. The model assumes there is no drift. | <input type="checkbox"/> | <input type="checkbox"/> |
| D. Linkage between a beneficial allele and hemophilia would have inflated Haldane's estimate of mutation rate for hemophilia. | <input type="checkbox"/> | <input type="checkbox"/> |

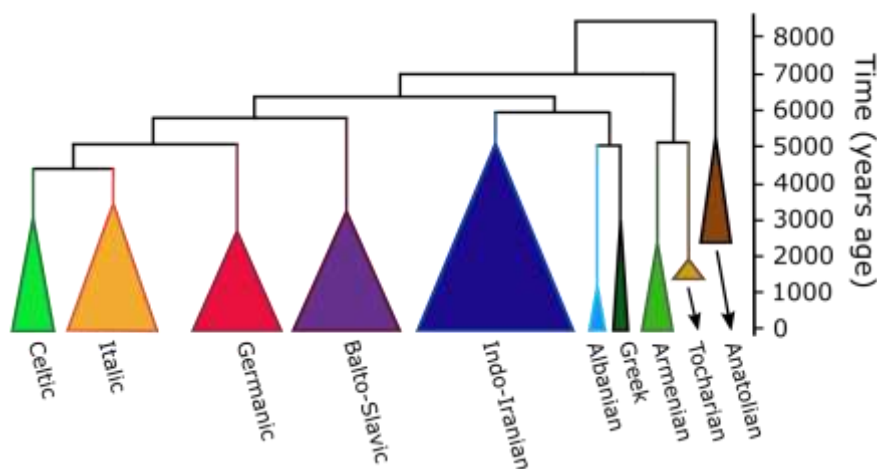
Q. 45 – Language Phylogeography

There are two hypotheses that try to explain the origin of the Indo-European language family.

The Steppe hypothesis traces back the origin of Indo-European language to the Pontic steppes region north of the Caspian Sea. Archaeological records provide some clues regarding to expansion from this area about 6000 years ago, however the implied models of such expansion remain untested.

Alternatively, it has been claimed that the languages spread from Anatolia with the development of agricultural activities about 8000 to 9500 years ago (the Anatolian hypothesis). The agricultural expansion reached the edge of Western Europe by 5000 years ago and had run its course about 4000 years ago.

Bouckaert and his colleagues (2018) assessed the two hypotheses with Bayesian phylogeographic approaches using vocabulary information from the ancient and contemporary Indo-European languages.



Maximum clade credibility tree indicating the divergence of the major Indo-European subfamilies. The tree demonstrates the timing of the appearance of the major branches and their subsequent variation. The area of each triangle represents the relative number of languages in each subfamily. Tocharian and Armenian are originated from steppe region.

- | | True | False |
|---|--------------------------|--------------------------|
| A. The result does not favour an Anatolian origin over a steppe origin. | <input type="checkbox"/> | <input type="checkbox"/> |
| B. It is unlikely that the spread of agriculture serves as the sole driver of language expansion on the continent. | <input type="checkbox"/> | <input type="checkbox"/> |
| C. Rate of language diversification in Balto-Slavic subfamily was higher than Germanic subfamily. | <input type="checkbox"/> | <input type="checkbox"/> |
| D. Drawing such trees is based on the assumption that languages does not affect each other when they come in contact. | <input type="checkbox"/> | <input type="checkbox"/> |

Q. 46 – Population Growth

The following data were collected by a researcher over seven successive years from a population of a fish in a pond. He calculated population growth rate (r) for each year using this formula

$$r = \ln N_{t+1} - \ln N_t$$

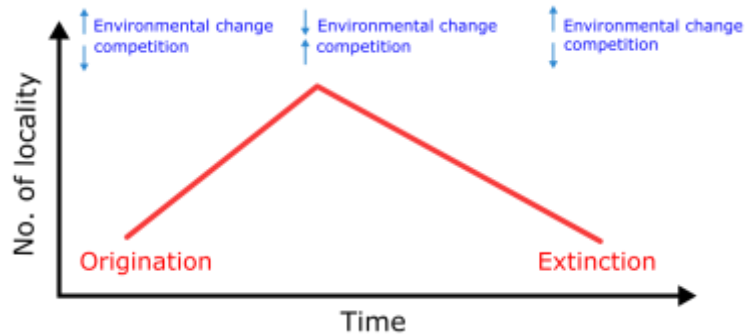
Note: N = the population size, K = the carrying capacity.

Year	Number of Fish	Population growth rate (r)
2002	2	2.77
2003	32	1.02
2004	89	-0.75
2005	42	0.39
2006	62	0.15
2007	72	-0.15
2008	62	-

- | | True | False |
|--|--------------------------|--------------------------|
| A. The fish population grows exponentially as r is bigger than 1 in all years. | <input type="checkbox"/> | <input type="checkbox"/> |
| B. When fecundity is less than mortality we can assume $N < K$, which means that the population is growing. | <input type="checkbox"/> | <input type="checkbox"/> |
| C. The fraction of the resources that were used by the fish in each year can be calculated by N/K . | <input type="checkbox"/> | <input type="checkbox"/> |
| D. The pond carrying capacity (K) is between 62 and 72. | <input type="checkbox"/> | <input type="checkbox"/> |

Q. 47 – Species Persistence

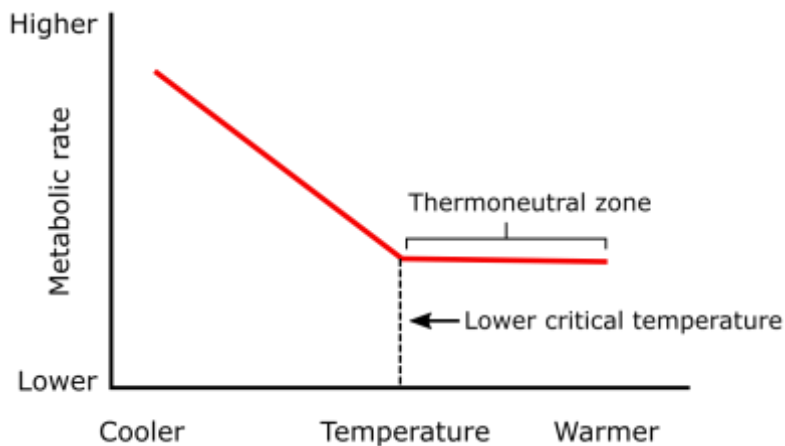
Žliobaitė *et al.* (2017) point out that for a given taxon, the pattern below is usually observed in the fossil record (red line) defined as the number of localities where a taxon is found. They propose that this pattern is a reflection of the evolutionary process, as shown by blue arrows representing the effects of environment and competition.



- | | True | False |
|--|--------------------------|--------------------------|
| A. According to the model the peak of a taxon's history is only identifiable after its extinction. | <input type="checkbox"/> | <input type="checkbox"/> |
| B. It has been observed that when different species reach their maximum population size in an island, competition and species richness is also at their maximum. This is consistent with the effect of environment and competition as shown in figure. | <input type="checkbox"/> | <input type="checkbox"/> |
| C. The extinction of a taxon should not depend on its age. | <input type="checkbox"/> | <input type="checkbox"/> |
| D. When a taxon is rare, its extinction is more likely to be the result of abiotic factors | <input type="checkbox"/> | <input type="checkbox"/> |

Q. 48 – Endothermy

Endotherm animals can only tolerate narrow range of body temperature (30–45 °C), but their ability to generate heat internally allowed them to expand their distributions. On the other hand, the cost to be endotherm is high because of their constant demand for food to support the energy needed for heat production.



- | | True | False |
|---|--------------------------|--------------------------|
| A. In a drastically-changing environment optimal body temperature of an endotherm animal will be largely maintained with minor behavioural adjustments. | <input type="checkbox"/> | <input type="checkbox"/> |
| B. When body temperature of endotherm animal starts dropping, it triggers the increase of metabolic heat generation, independent of animal habitat. | <input type="checkbox"/> | <input type="checkbox"/> |
| C. Basal metabolic rate of an endotherm animal stays constant throughout a limited range of environmental temperatures. | <input type="checkbox"/> | <input type="checkbox"/> |
| D. One way that some endotherm animal species tolerate extreme cold conditions is to alter their lower critical temperature. | <input type="checkbox"/> | <input type="checkbox"/> |

Q. 49 – Dynamics of Infectious Diseases

SIR model was developed by Kermack and McKendrick (1927) to explain dynamics of an infectious diseases. In this model, there are only three subgroups in the population including susceptible, infected, and recovered (S, I, and R respectively).

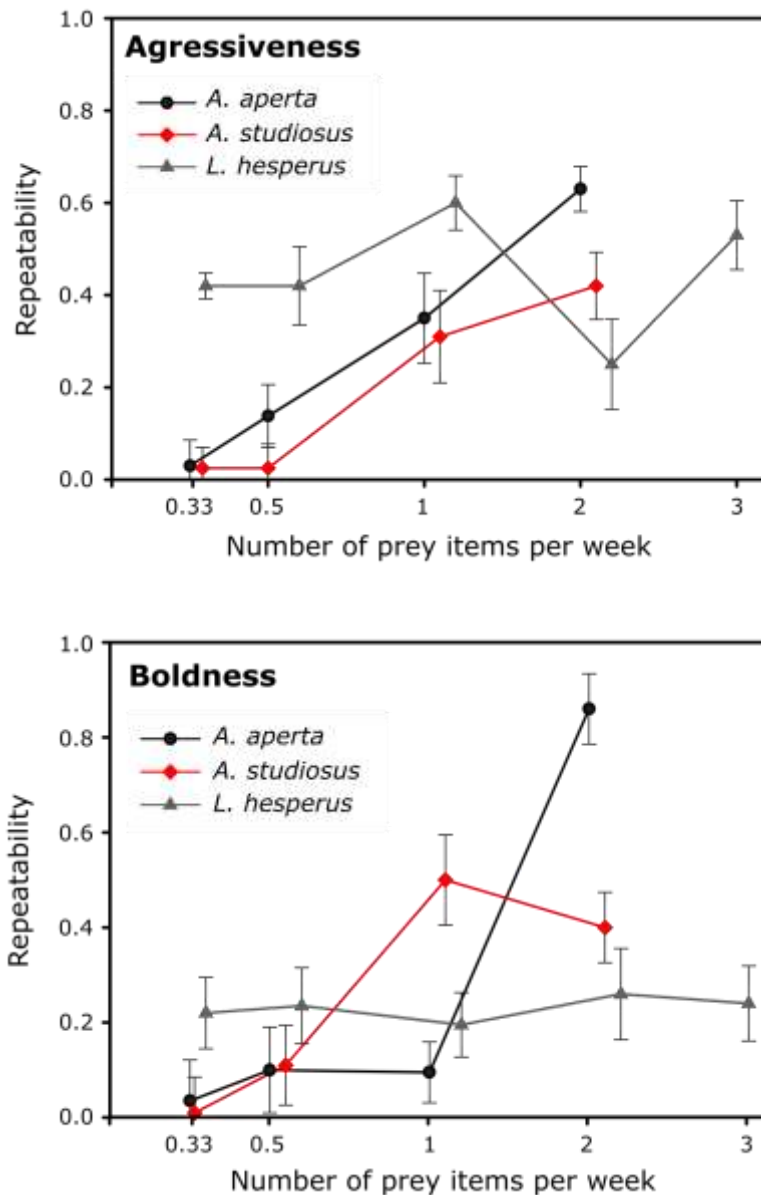
The model assumes that everyone is born susceptible and there is no passive immunity for the infants, everyone who recovers from the disease is immune, the probability of getting the infection is the same for every susceptible person, and people in each group die with their own per capita death rate (m_S , m_I , and m_R).

In this model, if a susceptible person contacts with an infected one, infection will be transmitted by probability of A and the rate of recovery is B .

- | | True | False |
|--|--------------------------|--------------------------|
| A. For the disease to remain in the population without adding any new source of infection, A should be at least equal to B . | <input type="checkbox"/> | <input type="checkbox"/> |
| B. The smaller the minimal infectious dose (the amount of pathogen required to cause an infection), the higher the A is. | <input type="checkbox"/> | <input type="checkbox"/> |
| C. If the disease is very lethal, it is more likely for it to be self-limited (the epidemic will finish all by itself). | <input type="checkbox"/> | <input type="checkbox"/> |
| D. If the infection period is longer, a higher proportion of population is infected. | <input type="checkbox"/> | <input type="checkbox"/> |

Q. 50 – Animal Personality

Animal personality is defined as individual differences in behaviour that are consistent across time and ecological context. One of the important drivers of personality difference is factors that alter the value of a decision. It was hypothesized that altering the feeding regimes of some spider species affect some aspects of their personality as you can see in graphs below.



Estimates of repeatability of boldness and aggressiveness response of three spider species under different feeding regimes. Error bars represent 95% confidence intervals for our repeatability estimates (After Lichtenstein, *et al.* 2016).

- | | True | False |
|--|--------------------------|--------------------------|
| A. This study failed to demonstrate association between boldness and aggressiveness regardless of feeding regimes. | <input type="checkbox"/> | <input type="checkbox"/> |
| B. Repeatability of aggressiveness response in <i>L. hesperus</i> is independent of feeding regimes. | <input type="checkbox"/> | <input type="checkbox"/> |
| C. Behavioural variation of each individual always decreases when spiders suffered prolonged food restrictions. | <input type="checkbox"/> | <input type="checkbox"/> |
| D. <i>L. hesperus</i> shows different repeatability in behavioural response than two other species regarding to different feeding regime, thus we can assume different species have different behaviour over time and contexts. | <input type="checkbox"/> | <input type="checkbox"/> |

Q. 51 – Parasitic Life Strategies

Sam is an imaginary single-celled organism. His body is covered with cilia which enable him to move. He has two nuclei: housekeeping genes are expressed in the macronucleus, while gene-expression tasks relevant to reproduction are undertaken by the micronucleus. Sam divides via a process called “schizogony”, whereby nuclei undergo multiple fission and then the cell itself divides. Sam can eat food particles and even bacteria through his mouth, a characteristic that helps him to live freely as a saprophyte. Sam has a monomorphic shape throughout its life cycle and experience enlargement and division, consecutively. Sam has decided to abandon his free-living lifestyle and transform into a merry parasite (with limited harm to the host).

Jack is also a parasite and is more aggressive (damages its host) than Sam and his single-celled body is covered by an armour made out of protein. This protective layer is jagged and gives Jack a rugged look. Jack also has two nuclei. He has two flagella that allows him to move, attack, and penetrate. He is able to secrete enzymes that can degrade many animal tissues. Immature individuals who belong to Jack's species lack traits mentioned above; they are small and proliferate rapidly. In addition, Immature individuals of Jack needs to find host to grow and cannot live independently.

- | | True | False |
|---|--------------------------|--------------------------|
| A. Utilizing antigen shuffling, even though it is a costly trait. | <input type="checkbox"/> | <input type="checkbox"/> |
| B. Having a life cycle consisting of two hosts. | <input type="checkbox"/> | <input type="checkbox"/> |
| C. Choosing an r-selected host. | <input type="checkbox"/> | <input type="checkbox"/> |
| D. Secreting <i>Samilosporin</i> (an antibiotic which destroys many of bacterial species that are virulent for the host). | <input type="checkbox"/> | <input type="checkbox"/> |
| E. Transmitting to the next generation by infecting the gametes. | <input type="checkbox"/> | <input type="checkbox"/> |

- | | True | False |
|--|--------------------------|--------------------------|
| A. Sam will probably win the competition against Jack. | <input type="checkbox"/> | <input type="checkbox"/> |
| B. If a lethal bacterium spread through the population of the host, Sam's fitness will increase. | <input type="checkbox"/> | <input type="checkbox"/> |
| C. Sam's fitness is negatively correlated with Jack's abundance. | <input type="checkbox"/> | <input type="checkbox"/> |
| D. Sam's fitness is less affected by the life-history traits of the host than Jack's. | <input type="checkbox"/> | <input type="checkbox"/> |

End
